

Genes Required for Osmoregulation and Apical Secretion in *Caenorhabditis elegans*

Samuel Liégeois,¹ Alexandre Benedetto, Grégoire Michaux,² Guillaume Belliard and Michel Labouesse³

Institut de Génétique et de Biologie Moléculaire et Cellulaire, Centre National de la Recherche Scientifique Institut National de la Santé et de la Recherche Médicale Université Louis Pasteur BP.10142, 67400 Illkirch, France

Manuscript received September 19, 2006
Accepted for publication November 23, 2006

ABSTRACT

Few studies have investigated whether or not there is an interdependence between osmoregulation and vesicular trafficking. We previously showed that in *Caenorhabditis elegans che-14* mutations affect osmoregulation, cuticle secretion, and sensory organ development. We report the identification of seven lethal mutations displaying *che-14*-like phenotypes, which define four new genes, *rdy-1*–*rdy-4* (rod-like larval lethality and dye-filling defective). *rdy-1*, *rdy-2*, and *rdy-4* mutations affect excretory canal function and cuticle formation. Moreover, *rdy-1* and *rdy-2* mutations reduce the amount of matrix material normally secreted by sheath cells in the amphid channel. In contrast, *rdy-3* mutants have short cystic excretory canals, suggesting that it acts in a different process. *rdy-1* encodes the vacuolar H⁺-ATPase α -subunit VHA-5, whereas *rdy-2* encodes a new tetraspan protein. We suggest that RDY-1/VHA-5 acts upstream of RDY-2 and CHE-14 in some tissues, since it is required for their delivery to the epidermal, but not the amphid sheath, apical plasma membrane. Hence, the RDY-1/VHA-5 trafficking function appears essential in some cells and its proton pump function essential in others. Finally, we show that RDY-1/VHA-5 distribution changes prior to molting in parallel with that of actin microfilaments and propose a model for molting whereby actin provides a spatial cue for secretion.

THE ability to control solute and water balance during osmotic challenge is essential for cellular life (YANCEY *et al.* 1982). Most cellular functions, in particular vesicle trafficking, depend on the specific balance of inorganic ions in the cytosol and the lumen. For instance, loss of the yeast endosomal Na⁺/H⁺ exchanger Nhx1 alters cytoplasmic and luminal pH, with profound consequences on the endocytic trafficking pathway (BRETT *et al.* 2005). In *Caenorhabditis elegans*, disruption of the epidermal chloride channel gene *clh-1* results in a significantly wider body and an abnormal structure of cuticular specializations called alae, which are secreted by the epidermis (PETALCORIN *et al.* 1999). Conversely, many animals and plants respond to the need to modify their internal ion balance by regulating the trafficking of certain ion transporters, channels, and exchangers. For instance, vasopressin triggers the fusion of sub-apical vesicles containing the aquaporin-2 membrane water channel with the apical plasma membrane of kidney-collecting-duct principal cells to mediate water excretion (NIELSEN *et al.* 1993, 1995). Although vesicle trafficking and osmoregulation seem interwoven,

whether or not there is a genetic basis for their interdependence is largely unclear.

An obvious approach to addressing this problem is to find mutations that would affect both osmoregulation and trafficking. In contrast to *Saccharomyces cerevisiae* for which a wealth of information on the genetic control of osmoregulation (HOHMANN 2002) or trafficking (SCHEKMAN and NOVICK 2004) is available, less is known about multicellular organisms. The nematode *C. elegans* provides many powerful experimental advantages for defining evolutionarily conserved genes, pathways, and mechanisms that give rise to diverse physiological processes (JORGENSEN and MANGO 2002). In particular, *C. elegans* has helped define genes that contribute to osmotic homeostasis (KAITNA *et al.* 2002; SOLOMON *et al.* 2004; LAMITINA and STRANGE 2005) and trafficking (NURRISH 2002).

We previously found that the *C. elegans* protein CHE-14 is important for both osmoregulation and apical trafficking (MICHAUX *et al.* 2000). A proportion of *che-14* larvae dies with an appearance of rods that are filled with fluid, which resemble larvae observed after laser ablation of the kidney-like excretory cell (NELSON and RIDDLE 1984). In addition, transmission electron microscopy (TEM) reveals that *che-14* mutants accumulate large vesicles in support cells of the amphid sensory organs and dark material at the apical surface of the epidermis, while the cuticle normally secreted apically is

¹Present address: UPR9022, IBMC, 67000 Strasbourg, France.

²Present address: UMR6061, CS 34317, 35043 Rennes Cedex, France.

³Corresponding author: IGBMC, 1 rue Laurent Fries, BP.10142, 67400 Illkirch, France. E-mail: lmichel@igbmc.u-strasbg.fr

much thinner than normal (MICHAUX *et al.* 2000). CHE-14 is homologous to Dispatched (MICHAUX *et al.* 2000), a protein required for the release of the Hedgehog morphogen in *Drosophila* (BURKE *et al.* 1999). However, the *C. elegans* genome lacks a canonical Hedgehog homolog and several additional components of the Hedgehog-signaling pathway, in particular Smoothed and Costal2, indicating that CHE-14 does not act in a Hedgehog-patterning process.

To address how CHE-14 might affect trafficking and osmoregulation, we sought to identify new genes acting in the same process. Here we report the results of a screen to uncover mutations displaying *che-14*-like phenotypes, which led to the identification of seven new mutations. These mutations define four genes that we call *rdy-1-4* (rod-like larval lethality and dye-filling defective), one of which corresponds to *vha-5* and codes for one of the four *C. elegans* α -subunits of the vacuolar H⁺-ATPase (V-ATPase) proton pump. The V-ATPase is a multisubunit protein complex consisting of two distinct subcomplexes: the cytosolic V1 complex that catalyzes ATP hydrolysis and the transmembrane V0 complex, to which VHA-5 belongs, that is responsible for proton translocation (NISHI and FORGAC 2002). While this work reports the actual molecular cloning of *rdy-1* as *vha-5*, we recently used *vha-5* mutations to show in a parallel study that the V0 sector of the V-ATPase is present at the limiting membrane of multivesicular bodies (MVBs) and at the epidermis apical membrane, where it allows the release of MVB internal vesicles (LIÉGEOIS *et al.* 2006). In particular, using hypomorphic mutations, we could genetically establish that VHA-5 has two distinct and separable functions—one involved in proton pumping within the entire V-ATPase complex and another involved in trafficking within the V0 complex alone (LIÉGEOIS *et al.* 2006). With this recent work as a background, here we molecularly characterize in parallel the genes *rdy-1/vha-5* and *rdy-2*, investigate their function in sensory organs, and compare the cellular role of *rdy-2* to that of *rdy-1/vha-5* in the epidermis. We also test which protein among RDY-1, RDY-2, and CHE-14 acts upstream of the other in the epidermis and in support cells. Finally, to extend our previous conclusions about the role of the V0 sector in cuticle secretion (LIÉGEOIS *et al.* 2006), we examine whether VHA-5 expression changes during molting, as observed for many genes involved in cuticle formation.

MATERIALS AND METHODS

***C. elegans* strains and maintenance:** *C. elegans* strains were handled and maintained at 20° as described previously (BRENNER 1974). The following strains were used: N2 (wild type); CB4856 (wild type); RW7000 (wild type); DH1206, *rme-8(b1023)* I; CB3823, *eDf18/unc-24(e138) dpy-20(e1282)* IV; KK627, *itDf2 V/nT1[unc-?(n754) let-?] (IV;V)*; MT3751, *dpy-5(e61)* I; *rol-6(e187)* II; *unc-32(e189)III*; MT464, *unc-5(e53)* IV; *dpy-11(e224)* V; *lon-2(e678)* X; *sqt-3(sc63) him-5(e1467) unc-*

76(e911); unc-24(e138) dpy-20(e1282); MT5813, *nDf42/nT1[unc-(n754)] IV; +/nT1 V*. CB4856 is an isolate from a Hawaiian island that shows a uniformly high density of polymorphisms compared with the reference Bristol N2 strain (<http://genomeold.wustl.edu/projects/celegans/index.php?snp=1>) (WICKS *et al.* 2001); RW7000 is a Bergerac strain with a high Tc1 copy number (WILLIAMS *et al.* 1992). Description of other strains, markers, and rearrangements can be obtained from WormBase (<http://www.wormbase.org>). Strains carrying genetic markers or deficiencies were obtained from the Caenorhabditis Genetics Center.

Mutagenesis and identification of *rdy* mutations: We previously described a trimethylpsoralen/UV (TMP/UV) clonal screen (MICHAUX *et al.* 2000), which was based on two steps: (i) identification of F₁ plates segregating rod-like larvae filled with fluid and (ii) staining of fluid-filled larvae that were still touch sensitive with the lipophilic dye 3, 3'-diocadecyloxycarbocyanine (DiO). DiO normally stains 12 amphid and phasmid sensory neurons, provided that their ciliated endings are normal and can access the environment through the channel formed by the surrounding socket and sheath cells (PERKINS *et al.* 1986). Staining with DiO was performed as described before (MICHAUX *et al.* 2000). Of 13,000 haploid genomes, 19 F₁ clones segregated dead rod larvae, among which 8 were DiO staining defective, including *che-14(mc35)* (MICHAUX *et al.* 2000); larvae with signs of necrosis under differential interference contrast (DIC) optics were discarded. These mutations, which defined four new complementation groups (*rdy-1-rdy-4*; see below), were outcrossed with N2 at least five times prior to further analyses. Their arrest stage was determined on the basis of the somatic gonad morphology, the migration/division of P cells, the division of seam and intestinal nuclei, and the appearance of postdeirid neurons.

Strong Ras pathway mutants (*let-60*, *mpk-1*, *let-23*, *sem-5*) also display a rod-like larval lethality (YOCHEM *et al.* 1997). We believe that *rdy* mutations do not affect the Ras pathway, as dying *let-23(sy10)*, *mpk-1(ku1)*, and *sem-5(n2019)* larvae could still take up DiO (data not shown).

Genetic mapping and complementation tests: Details about the assignment of *rdy* mutations to four complementation groups corresponding to *rdy-1(mc37)* and *rdy-1(mc38)* (LGIV), *rdy-2(mc39)* and *rdy-2(mc40)* (LGV), *rdy-3(mc41)* (LGIII), *rdy-4(mc42)* and *rdy-4(mc43)* (LGII) and their mapping can be found in the supplemental material at <http://www.genetics.org/supplemental/>.

Transgenesis and complementation rescue: DNA was injected into the syncytial gonads of hermaphrodites using injection mixes that generally contained 10 ng/ μ l construct or 100 ng/ μ l cosmid, 100 ng/ μ l pRF4 as a transformation marker (MELLO *et al.* 1991), plus pBSKII plasmid to bring the total DNA concentration to 200 ng/ μ l. DNA mixes were injected into *rdy-1(mc38)/unc-5(e53)* or *rdy-2(mc39)/sqt-3(sc63) him-5(e1467) unc-76(e911)* animals; rescue was judged on the absence of uncoordinated (Unc) animals in the progeny. For *rdy-1*, we found that *F35H10*, one of the two cosmids in the interval where *rdy-1* was predicted to map, could rescue the lethality of *rdy-1(mc38)*. RNA interference (RNAi) (FIRE *et al.* 1998) against *vha-5/F35H10.4*, which was known to be expressed in the excretory canal (OKA *et al.* 2001; PUJOL *et al.* 2001), indicated that *rdy-1* corresponds to *vha-5*. For *rdy-2*, we found that *C50B8*, *F53F4*, and a PCR fragment spanning *F53F4.4* and *F53F4.6* (10,785 bp; primers 5'-TGCTTCTGCCCTTCTC TCATTC and 5'-CATTTTCAGGACGAATACTTCC), but not PCR fragments spanning *F53F4.1* and *F53F4.2* (7773-bp fragment; primers 5'-GTCATAACAGCCTTAACTAC and 5'-GCATTTG TAGTGATTTCAAGG) or *F53F4.3* (4331-bp fragment; primers 5'-CGATGCTCCAATTAGTAAACC and 5'-CTTGCAACACTC GAAAGCTTG), could rescue the lethality of *rdy-2(mc39)*. After

digestion of the 10,785-bp PCR fragment with *Msd* or *Sall* and gel purification, the 6985-bp *Sall*-cut fragment containing only *F53F4.6*, but not the *Msd*-cut fragment containing *F53F4.4*, could rescue the lethality of *rdy-2(mc39)*. We conclude that *rdy-2* corresponds to the predicted gene *F53F4.6*.

RNA interference: Hermaphrodites were injected with double-stranded RNA transcribed with the message machine T3 kit (Ambion, Austin, TX) from a PCR fragment obtained with primers (5'-aattaaccctactaaaggGAGCTCTCTGAAGTCTTGTGG and 5'-aattaaccctactaaaggCAGAACTCAAAGAAA GAAGC; lowercase letters correspond to the T3 RNA *Pol* promoter) located in the 3'-end of *vha-5*. It induced a partial L2 larval lethality characterized by rod-like larvae filled with fluid.

DNA sequencing of *vha-5* and *rdy-2*: Using overlapping PCR reactions, we amplified the entire *vha-5* and *rdy-2* coding sequences and sequenced fragments bearing a deletion or all fragments for *rdy-2(mc39)*. *vha-5(mc37)* corresponds to a 214-bp deletion, including the genomic positions 2498–2711 downstream of the first *vha-5* coding nucleotide; *vha-5(mc38)* corresponds to a 124-bp deletion including the genomic positions 2298–2421 downstream of the first *vha-5*-coding nucleotide; *rdy-2(mc39)* corresponds to a T:A substitution at position 16,382 in the *F53F4* cosmid sequence and is predicted to transform an AGA codon into an opal stop codon; *rdy-2(mc40)* corresponds to a 121-bp deletion, including the positions 15,506–15,626 in the *F53F4* cosmid sequence.

RT-PCR in *rdy-2*: To determine the 5'-end of *rdy-2* transcripts, we used an RT-PCR strategy. Total RNA preparation and RT-PCR were carried out as described before (BOSHER *et al.* 2003). Reverse transcription was initiated with either oligo(dT) or 5'-ACGTAGAGAAGTGCTCCAAGG, which bridges the final two exons. PCR was done using the primer 5'-TACTTC TTCAAATCTCGACG or a primer corresponding to the sequence of the SL1 spliced leader and 5'-CAATGTGACACAGC TAACTCC (in the fourth exon) or the primer used for RT. RT-PCR products were then sequenced.

Fluorescent fusion proteins: Constructs were generated using standard procedures and subsequently transformed into XL1-blue electro-competent bacteria. The rescuing *vha-5::gfp* (pML670) and *vha-5::mrfp* (pML698) constructs are described elsewhere (LIÉGEOIS *et al.* 2006). Substituting the GFP-coding sequence with that of cyan fluorescent protein (CFP) (taken from plasmid pPD136.61, a kind gift from A. Fire, <http://www.ciwemb.edu/pub/FireLabInfo/>) produced the *vha-5::cfp* construct. pML680 (*Ex[+ΔHyp]*), carrying a 1542-bp deletion in the presumptive *vha-5* promoter, was obtained by digesting pML670 with *HindIII* and *AvrII* followed by T4 DNA polymerase treatment. Other *vha-5* promoter deletions were obtained by PCR using the primers 5'-aaaacgcgtgAGAAC TGTGAGAATTTCAATC and 5'-aaaacgcgtgAGGTGTTAAAG GCTAATCTGC (deletion 1493–2494; underlined sequence, *MluI* site) and 5'-aaaacgcgtgACAGTTCTCAATTCATATTGG and 5'-aaaacgcgtgATCTCTCCTTTGTTGCTC (deletion 2482–2652) starting from pML670. pML673, encoding a RDY-2::GFP functional fusion protein, was obtained by cloning the promoter and the full-length coding sequence of *F53F4.6* in frame with the GFP-coding sequence (primers 5'-cccagagctc GACAAGAAACGTGTTTCGAGC, *SadI* underlined, and 5'-gggg taccAACTTTTCACGAGATATGAAGATTA, *KpnI* underlined) in a modified version of pPD95.75 in which a *Sad* site had been engineered. Substituting the GFP-coding sequence with that of CFP produced the *rdy-2::cfp* construct. A similar strategy was used to generate a *che-14::yfp* construct starting from the previously described *che-14::gfp* construct (MICHAX *et al.* 2000). To examine the distribution of RDY-2 and CHE-14 mutants in weak *rdy-1* mutants, we co-injected the selection marker pRF4 with the mutant *vha-5(L786S)::mrfp* transgene (at 3 ng/μl)

(LIÉGEOIS *et al.* 2006) with *rdy-2::cfp* (at 5 ng/μl) and *che-14::yfp* (at 20 ng/μl) constructs in *vha-5(mc38)/unc-5(e53)* animals and selected F₂ transgenic animals that did not segregate Uncs. To generate the *vha-8_p::vab-10_{ABD}::yfp* construct, the *vha-8* promoter (primers 5'-aaaagtggtaccAAAGTATTGTCGG CAAGGCAC and 5'-tccccgtgaccAGTCGTTAGTGGTTTC CCTG; *KpnI* underlined) was cloned upstream of a cDNA encoding the first 290 residues of the spectraplakins VAB-10 (BOSHER *et al.* 2003) fused to the yellow fluorescent protein (YFP)-coding sequence in the pPD136.64 vector (kind gift from A. Fire, <http://www.ciwemb.edu/pub/FireLabInfo/>). This construct and the *vha-5::cfp* plasmid (see above) were co-injected with or without a *dlg-1::rfp* plasmid marking the *C. elegans* adherens junction (gift from Jeff Hardin); at least three animals for each larval stage from more than two independent transgenic lines were examined and gave identical results.

Mosaic analysis of *vha-5*: Mosaic analysis of *vha-5* was performed using two parallel strategies. In the first case, homozygous transgenic *vha-5(mc38); Ex[pML670]; pRF4* animals were allowed to lay eggs for 6–8 hr (pML670 is a rescuing *vha-5::gfp* construct; see above). Rdy dead larvae were examined by DIC and GFP fluorescence 24 hr after egg laying; plates were also inspected over the next 2 days for rare dying larvae that could progress beyond the L2 stage. In the second case, we induced deletions in the *vha-5* promoter by generating three plasmids: pML680 was obtained by digesting pML670 with *HindIII* and *AvrII* followed by T4 DNA polymerase treatment (1542-nt deletion); pML685 and pML689 were obtained by PCR to amplify the plasmid pML670 except the promoter region encompassing nucleotides 1494–2494 (primers 5'-aaaacgcgtgAGAACTGTGAGAATTTCAATC and 5'-aaaacgcgtg AGGTGTTAAAGGCTAATCTGC) or nucleotides 1494–2653 (primers 5'-aaaacgcgtgACAGTTCTCAATTCATATTGG and 5'-aaaacgcgtgATCTCTCCTTTGTTGCTC), respectively; the underlined *MluI* restriction site was used for religation.

Microscopy: DIC, TEM, scanning electron microscopy (SEM), and confocal microscopy were performed as described elsewhere (LIÉGEOIS *et al.* 2006). TEM on *rdy* mutants was carried out by picking larvae as soon as signs of rigidity and translucence became apparent, which was <32 hr after egg laying. TEM and SEM on adults were done by picking L4 larvae 24 hr prior to fixation. For TEM, four *vha-5(mc38)* and three *rdy-2(mc39)* animals were observed. For both *vha-5(mc38)* and *rdy-2(mc39)* animals, a set of at least 20 adjacent ultrathin sections from the tip of the head and at least three sections taken in at least three different areas of the body were analyzed. For SEM, 15 animals were observed for the *vha-5(mc38); Ex[pML680]* strain, which all displayed alae defects.

RESULTS

A genetic screen for mutants displaying *che-14*-like phenotypes: *che-14* larvae display two phenotypes that are easy to score (MICHAX *et al.* 2000). First, a proportion of *che-14* larvae die looking as rods filled with fluid. Second, all *che-14* L2 and older larvae display a dye-staining defect of amphid and phasmid chemosensory neurons after incubation with the lipophilic dye DiO. DiO normally stains neuronal cell bodies, provided that their ciliated endings are normal and have access to the environment through the channel formed by the surrounding socket and sheath cells (PERKINS *et al.* 1986).

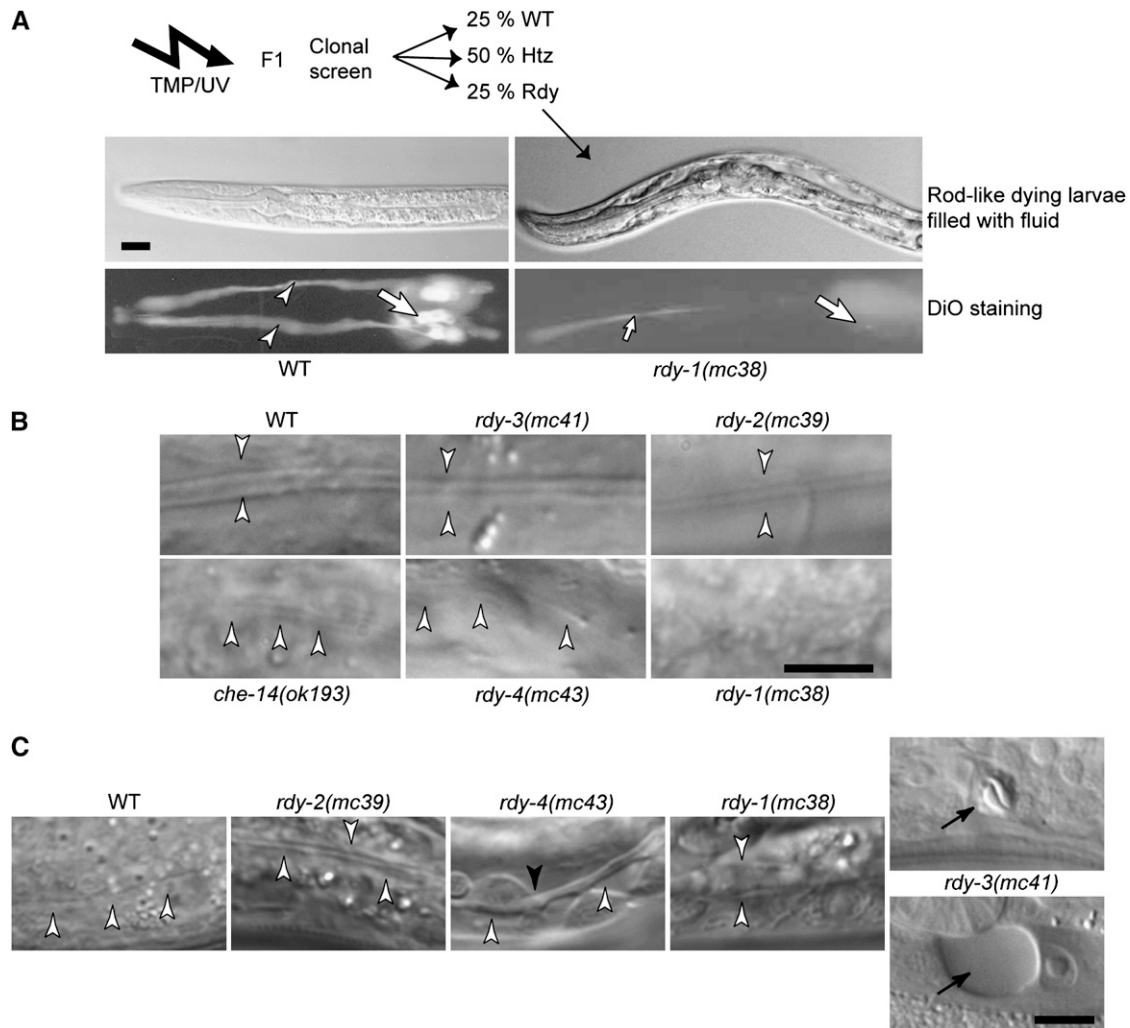


FIGURE 1.—Mutagenesis and identification of *rdy* mutations. (A) Strategy for the identification of *rdy* mutations. After TMP/UV mutagenesis, the progeny of individual F₁ animals were examined for the presence of rod-like larvae filled with fluid (top photos: DIC microscopy) and then for staining with the lipophilic dye DiO (bottom photos: fluorescence microscopy), which normally labels 12 neurons in the head (large arrows) and their dendrites (arrowheads). (Left) Wild-type (WT) larvae. (Right) *rdy-1(mc38)* mutants (the small arrow in the bottom photo points to the pharyngeal lumen). (B) L1 larva alae (arrowheads) of wild-type and *rdy* mutants viewed by DIC microscopy. Larvae are arranged in order of increased severity from WT = *rdy-3* (normal alae) > *rdy-2* > *che-14* = *rdy-4* > *rdy-1* (no alae). (C) Excretory canal (open arrowheads) of L1 larvae viewed by DIC microscopy and arranged in order of increased severity: the canal was thicker in *rdy-2* mutants; thicker and irregular (solid arrowhead) in *rdy-4* mutants; extremely thick in *rdy-1* mutants; essentially absent in *rdy-3* mutants, in which vacuoles (arrow) that progressively grew in size (top—24 hr after egg laying; bottom—32 hr after egg laying) could be seen at the level of the excretory cell body. Bars, 5 μ m.

To identify essential as well as nonessential genes potentially acting in the same process as *che-14*, we used a two-step clonal strategy with the two criteria described above (Figure 1A). This screen led to the identification of *che-14(mc35)* (MICHAX *et al.* 2000). We also recovered seven other mutations (not described at the time), named *mc37–mc43*. We completed this screen by a closer examination of the cuticle, as *che-14* adults have stunted alae, which are cuticular specializations running along the lateral side of the animal (Figure 1B). We called the genes identified by these mutations *rdy*. Genetic analysis showed that they define four complementation groups, which mapped onto four chromosomes (see supplemental material at <http://www.genetics.org/supplemental/>).

The gene *rdy-3* is defined by a single allele, and the others by two alleles.

Table 1 and Figure 1 present a more detailed account of the defects conferred by the *rdy* mutations. First, whereas *che-14* mutants display a partial larval lethality, other *rdy* mutations induced a fully penetrant lethality during the L1 or L2 larval stages. Since all known *che-14* mutations are strong or null alleles (MICHAX *et al.* 2000), some essential functions carried by *rdy* genes must be *che-14* independent. Second, they all displayed a penetrant dye-filling defect in amphids and phasmids, as do *che-14* alleles. Third, DIC microscopy suggested that all *rdy* L1 larvae, except *rdy-3(mc41)*, had abnormal alae (Figure 1B); the alae defect of *che-14* larvae was

TABLE 1
Phenotypes of the *rdy* mutants

Genotype	% Rdy (N) ^a	Stage of lethality ^b	DiO(+) neurons ^c	Alae ^d
Wild type	0	—	10.5 ± 1 (n = 20)	+++
<i>che-14(mc35)</i>	49 (n = 305)	L1 to adult	1.2 ± 1 (n = 20)	+
<i>rdy-1(mc37)</i>	21 (n = 241)	Mid-L1 (n = 18)	1.1 ± 2.2 (n = 24)	—
<i>rdy-1(mc38)</i>	24 (n = 228)	Mid-L1 (n > 50)	1.5 ± 2.7 (n = 13)	—
<i>rdy-2(mc39)</i>	23 (n = 245)	L2 (n > 50)	1.1 ± 2.1 (n = 10)	++
<i>rdy-2(mc40)</i>	22 (n = 262)	L2 (n = 21)	1.3 ± 2 (n = 21)	++
<i>rdy-3(mc41)^e</i>	21 (n = 571)	90% L2/10% L3 (n = 38)	0 (n = 20)	+++
<i>rdy-4(mc42)</i>	22 (n = 380)	Mid-L1 (n = 25)	0 (n = 10)	+
<i>rdy-4(mc43)</i>	23 (n = 248)	Mid-L1 (n > 50)	1.2 ± 1 (n = 20)	+

^a Percentage of rod-looking larvae filled with fluid in the progeny of heterozygous *rdy* mutant strains or in the progeny of homozygous *che-14(mc35)* animals. Although the proportion of Rdy larvae was always <25%, we believe that their lethality is fully penetrant, as their transparency makes them difficult to spot and as we never recovered viable adults laying only Rdy larvae.

^b Stage when larvae ceased to move, which was assessed at least 48 hr after egg laying.

^c No. of amphid chemosensory neurons that were stained by DiO, which can normally stain 12 neurons in wild-type animals.

^d Presence or absence of alae under DIC microscopy with an arbitrary score ranging from +++ to — (see Figure 1C).

^e *rdy-3(mc41)* larvae were frequently found to die off food, which is a further indication that they have defective chemosensory organs.

intermediate between those of *rdy-1* and *rdy-2*; that of *rdy-4* larvae was slightly variable but generally like that of *che-14* larvae. In wild-type animals, the excretory cell sends out long anterior and posterior processes, which run on both sides of the animal and are called the excretory canals. The posterior canals extend until the somatic gonad at the L1 stage and reach the rectum in L2 larvae. *rdy-1*, *rdy-2*, and *rdy-4* mutants had an excretory canal of normal length, but it was abnormally wide and occasionally exhibited swelled areas (Figure 1C). In contrast, *rdy-3(mc41)* larvae had no excretory canal and developed a progressive vacuole at the level of the excretory cell body (Figure 1C; 21 of 29 had no canal; 6 had a canal extending up to the position of the H2 blast cell, and 2 until the position of the V1 blast cell). We thus suggest that *rdy-3* may act in a different process than the other *rdy* genes.

We decided to focus on *rdy-1* and *rdy-2*, which had strong alae phenotypes. Our *rdy-1* and *rdy-2* alleles are strong loss-of-function or null alleles, since their phenotypes did not worsen in *trans* to deficiencies (see MATERIALS AND METHODS). For simplicity, we will first describe their cloning and then their cellular phenotypes.

RDY-1 corresponds to the V-ATPase α -subunit VHA-5: To determine the molecular identity of *rdy-1*, we used a classical strategy combining high-resolution genetic mapping, RNA interference, and transgene-mediated complementation rescue (Figure 2A) (see MATERIALS AND METHODS). We found that *rdy-1* corresponds to the previously described gene *vha-5* (OKA *et al.* 2001; PUJOL *et al.* 2001) (Figure 2A). In particular, we found that *rdy-1(mc37)* and *rdy-1(mc38)* are small deletions in *vha-5*,

which induce premature stop codons (Figure 2B). This result is consistent with the nature of the mutagen used (trimethylpsoralen), the genetic tests showing that *mc37* and *mc38* are strong or null alleles (see supplemental material at <http://www.genetics.org/supplemental/>), and the absence of wild-type VHA-5 in Western blots of *vha-5(mc38)* animals (LIÉGEOIS *et al.* 2006). Below, we will refer to *rdy-1* as *vha-5*. VHA-5 corresponds to one of the four *C. elegans* large transmembrane subunits of the V-ATPase, the so-called α -subunit. VHA-5 and the other α -subunits (UNC-32, VHA-6, and VHA-7) have specific tissue distributions (OKA *et al.* 2001; PUJOL *et al.* 2001). The V-ATPase is involved in acidification of secretory and endocytic organelles and is essential for osmoregulation in animal excretory systems (NISHI and FORGAC 2002; SUN-WADA *et al.* 2003). The transmembrane V0 sector, to which VHA-5 belongs, also plays a direct role in trafficking in yeast, *Drosophila*, and *C. elegans* (PETERS *et al.* 2001; BAYER *et al.* 2003; HIESINGER *et al.* 2005; LIÉGEOIS *et al.* 2006).

***rdy-2* encodes a four-transmembrane protein of unknown function:** Using a similar strategy, we showed that the predicted gene *F53F4.6* could rescue the lethality of *rdy-2(mc39)* larvae (see MATERIALS AND METHODS and Figure 3A). In particular, we found that the mutation *rdy-2(mc39)* changes the Arg codon 71 into an opal stop codon, whereas *rdy-2(mc40)* is a deletion inducing a frameshift (Figure 3, B and C; supplemental Figure 1 at <http://www.genetics.org/supplemental/>), in agreement with the prediction that both are strong or null alleles (see supplemental material at <http://www.genetics.org/supplemental/>). RT-PCR experiments and sequence comparisons, which are further detailed in

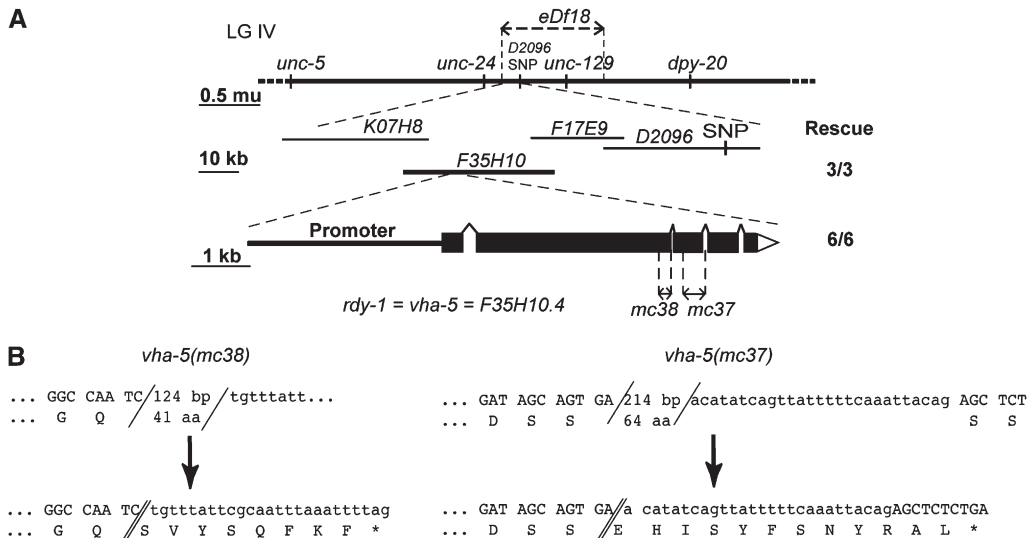


FIGURE 2.—*rdy-1* corresponds to *vha-5* and codes for a V-ATPase α -subunit. (A, top). Genetic map of chromosome IV showing the positions of markers used to map *rdy-1*. *rdy-1(mc37)* and *rdy-1(mc38)* mutations were positioned between the left breakpoint of *eDf18*, which is defined by cosmid *K07H8*, and a SNP located in cosmid *D2096*. (Middle) Among cosmids in this region, *F35H10* rescued the lethality of *rdy-1(mc38)* larvae (number of rescued lines indicated on the right). (Bottom) RNAi and further rescuing tests proved that *rdy-1* corresponds to the gene *F35H10.4/vha-5*, whose exon-intron structure is shown along with the positions of *mc37* and *mc38*. (B) More detailed description of the molecular lesions corresponding to *vha-5(mc38)* and *vha-5(mc37)*. (Top) Wild-type sequence flanking the deletion breakpoints (slashes). (Bottom) Mutant sequence and distance to the nearest stop codon.

supplemental Figure 1 at <http://www.genetics.org/supplemental/>, suggest that there are two distinct *rdy-2* transcripts with distinct 5'-ends. The long and short *rdy-2* transcripts potentially encode two tetraspan membrane proteins (Figure 3D; supplemental Figure 1 at <http://www.genetics.org/supplemental/>) with predicted N- and C-terminal cytosolic tails. Many nematode species, including the distant parasitic nematodes *Meloidogyne incognita* and *Strongyloides stercoralis* (<http://www.nematode.net/blast>), encode homologs of the short RDY-2 isoform, but only the closely related *C. briggsae* and *C. remanei* species are predicted to encode homologs of the long RDY-2 isoform (supplemental Figure 1B at <http://www.genetics.org/supplemental/>). It suggests that the short RDY-2 isoform might carry the most important function. Outside of nematodes, there are no RDY-2 homologs. In particular, the sizes and sequences of RDY-2 extracellular and cytosolic loops differ from those of other tetraspan proteins, such as proteolipids, connexins, tetraspanins, and claudins. Nonetheless, we note that these well-characterized tetraspan proteins are involved in cell adhesion, membrane integrity, or possibly apical trafficking (CHEONG *et al.* 1999).

***vha-5* and *rdy-2* mutations affect osmoregulation and secretion:** As outlined above, *rdy* mutants share with *che-14* mutants several phenotypes at the level of the dissecting microscope. To determine whether this could also be the case at the subcellular level, we examined *vha-5(mc38)* and *rdy-2(mc39)* larvae by transmission electron microscopy as they were becoming rods.

Excretory cell: In wild-type animals, a system of beaded canaliculi feed into a central apical lumen of the excretory canal (Figure 4A), which is surrounded by a basal lamina that it shares with the neighboring epidermis. Typically, in *che-14* mutants the excretory canal is

poorly attached and frequently enlarged (MICHAUX *et al.* 2000). In agreement with the DIC analysis (Figure 1) and with the characterization of point mutations partially affecting the proton pump function of *vha-5* (LIÉGEOIS *et al.* 2006), we found that *vha-5(mc38)* null larvae and, to a lesser extent, *rdy-2* mutant larvae had an enlarged excretory canal (Figure 4A).

Epidermis: The epidermis secretes the cuticle (Figure 4B), which in L1, dauer, and adult stages forms alae with contributions from seam cells and the hyp7 syncytial epidermis (SAPIO *et al.* 2005). Typically, *che-14* mutants have a thinner cuticle and alae. We could detect both epidermal and cuticular defects in *vha-5* null larvae (Figure 4, B and C). Within the epidermis, we noted that the stacked sheets of membranes, which normally invaginate from the apical membrane, were either reduced in size or disorganized (Figure 4B, open arrowhead). Extracellularly, the cuticle had an abnormal structure (Figure 4, B and C). In some places, dense material accumulated under the cuticle (Figure 4C), while in others the cuticle was not closely apposed to the epidermal apical plasma membrane (Figure 4B, solid arrowhead). The cuticle's outer surface was wavy instead of flat, it had an irregular thickness, and alae were absent (Figure 4C) (consistent with the DIC phenotype). The apparent separation between the epidermis and the cuticle might reflect an osmoregulation defect; the structural cuticular defects are consistent with the observation that point mutations partially affecting the trafficking function of VHA-5, but not its proton pump function, had reduced alae and were dumpy (LIÉGEOIS *et al.* 2006). The cuticle of *rdy-2* larvae was abnormal, too, but not as severely affected: its most distinctive feature was the irregular and generally flattened structure of its alae (Figure 4C).

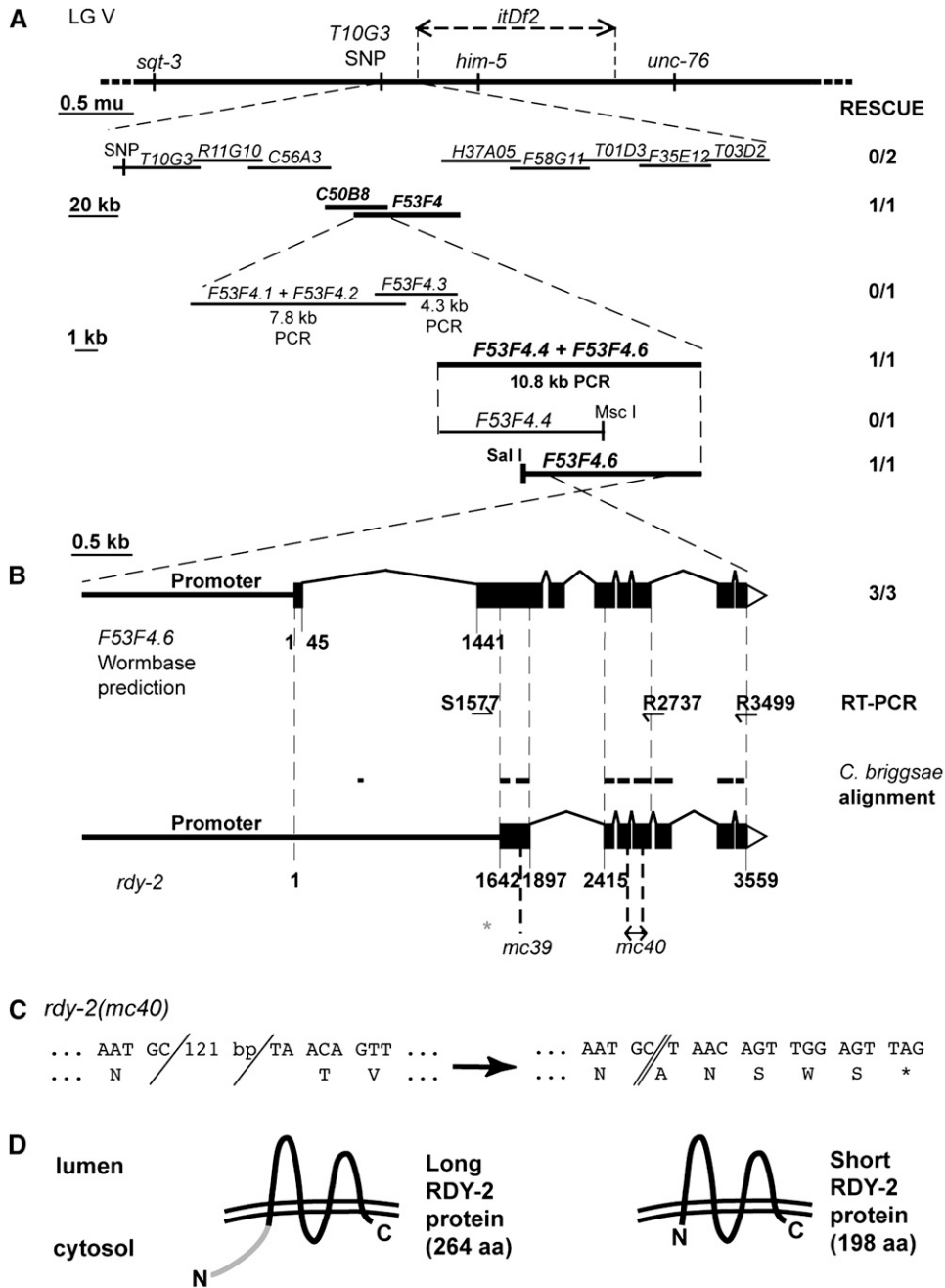


FIGURE 3.—*rdy-2* encodes two putative tetraspan proteins. (A, top) Genetic map of chromosome V showing the positions of markers used to map *rdy-2*. *rdy-2(mc39)* and *rdy-2(mc40)* mutations were positioned between a SNP localized in the cosmid *T10G3* and the left breakpoint of *itDf2*, which is defined by the cosmid *T03D2*. (Middle) Among cosmids in the area, only cosmids *C50B8* and *F53F4* (boldface type) could rescue the lethality of *rdy-2(mc39)* larvae (the number of rescuing lines tested for the presence of cosmid DNA by PCR is indicated on the right). (Bottom) Among PCR-generated subfragments of *F53F4*, only *F53F4.6* could rescue the lethality of *rdy-2(mc39)* larvae. (B) Predicted exon–intron structure of *F53F4.6* according to Wormbase version WS157 (top) and actual exon–intron structure of *rdy-2* transcripts deduced from RT–PCR experiments using the primers symbolized between both structures (half arrows; S, sense; R, reverse; nucleotides are numbered relative to the first AUG according to WS157). The positions of conserved areas in the *C. briggsae* *F53F4.6* homolog are symbolized by dashed lines. (C) A more detailed description of the molecular lesion corresponding to *rdy-2(mc40)* (see Figure 2B for symbols). (D) Topology of the long and short RDY-2 proteins as predicted by the software TMHMM version 2.0 (<http://www.cbs.dtu.dk/services/TMHMM/>); the N-term extension of the long protein is indicated shaded.

Chemosensory organs: In wild-type animals, the bilateral amphid ciliated neurons go through two consecutive channels made by the amphid sheath and the amphid socket cells (Figure 5A), both of which are affected in *che-14* mutants (PERKINS *et al.* 1986; MICHAUX *et al.* 2000). The bilateral amphid sheath cells, and several other sensory neuron sheath cells, contain distinctive parallel membrane lamellae (Figure 5B, right enlargement), which are suspected to play a role in the formation of the large vesicles that are secreted within the amphid pocket and accumulate in *che-14* mutants (PERKINS *et al.* 1986). The content of these vesicles might correspond to the granular electron dense

material surrounding the ciliated endings of chemosensory neurons (PERKINS *et al.* 1986) (Figure 5D, enlargement). In *vha-5* null larvae, these lamellae adopted a circular ring-like structure (Figure 5C, arrowheads). At a slightly posterior level, neurons were separated in an abnormally wide and electron-light lumen (Figure 5E), and we noted an absence of granular material around neurons in the amphid pocket (Figure 5E, arrowhead). Enlargement of the sheath pocket might also reflect an osmoregulation defect. Likewise, in *rdy-2* mutant larvae, we could not find any granular material around neurons, which were also spread out in an abnormally wide electron-light lumen (Figure 5F, arrowhead). These

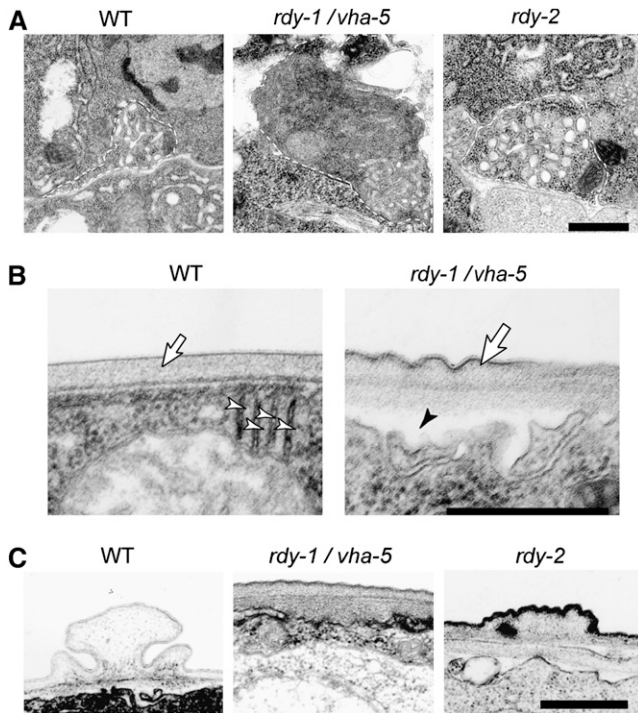


FIGURE 4.—*vha-5* and *rdy-2* mutants have enlarged excretory canals and cuticle secretion defects. TEM images of wild-type (WT), *vha-5(mc38)*, and *rdy-2(mc39)* L1 larvae. (A) Cross section through the excretory canal; its outline is marked by a dashed line. Note the enlarged section of the canal in *rdy* mutants and its dark appearance in the *rdy-1/vha-5* larva. The average canal section was $0.22 \pm 0.05 \mu\text{m}^2$ in wild-type L1 larvae, $0.69 \pm 0.31 \mu\text{m}^2$ in *vha-5(mc38)* larvae ($P < 0.0005$), and $0.44 \pm 0.11 \mu\text{m}^2$ in *rdy-2(mc39)* larvae ($P < 0.0001$). (B) Cross section through the epidermis. In *vha-5(mc38)* larvae, stacked sheets of membrane (arrowhead) originating from the apical plasma membrane are irregular, and the cuticle is irregular (arrow) and has partially detached from the epidermis (solid arrowhead). (C) The alae of the *vha-5(mc38)* larva are absent, and those of the *rdy-2(mc39)* larva have a flat structure, compared to control alae. Bars, $0.5 \mu\text{m}$.

defects are compatible with a direct or indirect (see DISCUSSION) role in secreting the granular material found in the amphid channel and in controlling osmoregulation in the amphid pocket.

***vha-5* acts cell-autonomously:** The early larval lethality and strong excretory cell defects of *vha-5* mutants raise the prospect that the cuticle secretion defects might be indirect and result from lethality. To test this possibility, we performed a mosaic analysis of *vha-5* using two parallel approaches that both rely on the use of a rescuing *vha-5* transgene expressed in the excretory cell and the epidermis (LIÉGEOIS *et al.* 2006) (see also below). First, we analyzed the defects observed in dead larvae segregating from transgenic *vha-5(mc38)* animals carrying a rescuing *vha-5::gfp* transgene. Second, we sought to rescue *vha-5* function in the excretory canal but not in the epidermis. Using the first approach, we found that larval lethality is due mainly to loss of *vha-5* expression in the excretory system, since all Rdy larvae

had lost *vha-5::gfp* expression in the excretory system (Table 2). However, larvae retaining expression in the epidermis (class I and II) could survive longer than Rdy larvae with no expression at all (class III), implying that the epidermis also requires VHA-5 function to maintain the animals' health (Table 2). To specifically rescue *vha-5* function in the excretory cell, we used promoter deletions in the *vha-5* promoter, as we could not find any well-characterized gene expressed in the excretory system but not in the epidermis (Figure 6A). One *vha-5* promoter deletion (*vha-5; Ex[Δhyp]*) remained active in all cells expressing *vha-5*, except in the epidermis after the L4/adult switch, and rescued the larval lethality of *vha-5(mc38)*. The corresponding adults displayed thinner alae than wild-type adults and their cuticle was not closely apposed to the epidermis everywhere when examined by electron microscopy (Figure 6, B and C), as also observed in *vha-5* null mutants (Figure 4, B and C). Collectively, these data show that *vha-5* acts cell-autonomously and that the cuticle defects do not result from the absence of VHA-5 function in the excretory system.

VHA-5 and RDY-2 are apical and have overlapping distributions: To further define the roles of *rdy-1/vha-5* and *rdy-2*, we determined their expression patterns using functional translational fusions (see Figures 2 and 3). Using GFP constructs and antibodies, we previously showed that VHA-5 is expressed in the excretory canal and the epidermis (LIÉGEOIS *et al.* 2006). We found that RDY-2 has a distribution very similar to that of VHA-5 in these tissues (Figure 7A). Specifically, we saw expression in the lining of the excretory canal and excretory duct, but not around the excretory pore. As no expression was seen around the excretory cell body, we conclude that RDY-2 is localized at the apical side of the canal, as reported for VHA-5 (LIÉGEOIS *et al.* 2006). RDY-2 had a distribution in the epidermis similar to that of VHA-5 and was also excluded from seam cells (Figure 7A). In contrast to VHA-5, whose expression was observed throughout development, starting at midembryogenesis, RDY-2 expression became progressively fainter after the L1 stage. VHA-5 was also detected at the lumen of the vulva and rectum (data not shown). In addition, we found that VHA-5 as well as RDY-2 were expressed in the sheath cells associated with head and tail sensory organs (Figure 7A). Three-dimensional reconstructions showed that VHA-5 and RDY-2 formed a sixfold symmetrical pattern, which includes a larger spot that presumably corresponds to the amphid (Figure 7C). We thus suggest that RDY-2 and VHA-5 are present in CEP and/or OLQ support cells, in addition to amphid support cells. In the amphid sheath cell, VHA-5 and RDY-2 were found in the most distal part of the cell lining the sheath pocket, which can be equated to its apical side (Figure 7, C and D). Expression in the excretory system, in sheath cells, and in the epidermis matches well *vha-5* and *rdy-2* phenotypes, strengthening the notion that these genes act cell-autonomously.

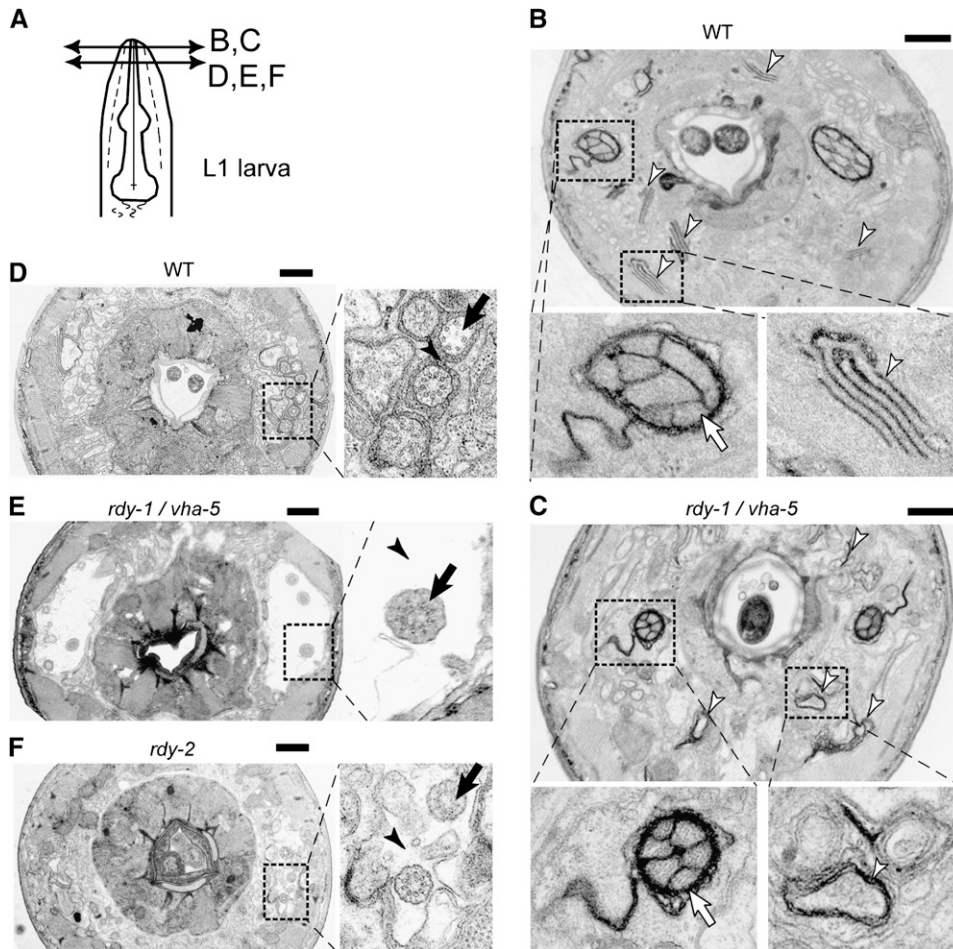


FIGURE 5.—VHA-5 and RDY-2 are essential for secretion of matrix material by sheath cells. (A) Schematic showing the approximate positions of the different TEM transverse sections in B–F. All images correspond to L1 larvae. (B) Wild-type (WT) and (C) *vha-5(mc38)* larvae, close to the tip of the nose. The left and right magnifications show the amphid opening at the level of the socket channel (arrow, terminal sensory dendrites) and a stack of membrane sheets (arrowhead), respectively; amphid neurons were normally enclosed by the socket channel in *vha-5(mc38)* mutants, but membrane sheets were disrupted (arrowhead). (D) Wild-type, (E) *vha-5(mc38)*, and (F) *rdy-2(mc39)* larvae, further posteriorly, showing ciliated neurons surrounded by the amphid sheath. Note in the enlarged view (right), the dark material (arrowhead in D) in the extracellular space around ciliated dendrites (arrow), which is absent in the two *rdy* sections. Instead, there is empty space around the dendrites (arrowheads), particularly in the *vha-5* larva. Bars, 1 μ m.

***vha-5* acts upstream of *che-14* and *rdy-2* in epidermal but not in sheath cells:** Our initial goal was to identify genes acting in the same process as *che-14* in osmoregulation and trafficking. To test if this was the case for *vha-5* and *rdy-2*, we reasoned that they should have, at a minimum, the same subcellular distributions as *che-14* and possibly be mutually required for their localization. We generated a triple transgenic line expressing functional VHA-5::mRFP, RDY-2::CFP and CHE-14::YFP constructs. Three-dimensional reconstructions through the head showed that CHE-14 was uniquely present in socket cells (green area in Figure 7D). This observation, along with the absence of RDY-2 and VHA-5 from seam cells, indicates that CHE-14 can work independently of VHA-5 and RDY-2 at least in some cells. We noted that RDY-2 was enriched in the anterior- and posterior-most areas of the amphid sheath cell surrounding the sheath pocket compared to CHE-14 or VHA-5 (YZ sections of Figure 7D); the significance of this enrichment is unclear. We next looked at the distribution of the three same transgenes in a weak *vha-5* mutant background, which was obtained by rescuing the *vha-5(mc38)* null mutant with a *vha-5* transgene carrying the point mutation L786S. This mutation affects the trafficking function of VHA-5, causing the fusion protein and some cargoes to

accumulate within dark MVBs in the epidermis (LIÉGEOIS *et al.* 2006). We found that CHE-14 and RDY-2 colocalized with the mutant VHA-5 in the epidermis (Figure 7B), presumably within MVBs. We conclude that VHA-5 is required for a late trafficking step of CHE-14 and RDY-2 in the epidermis. In contrast, the distributions of the three proteins in sensory organs were overall quite similar to that observed in control heterozygous animals (Figure 7D). In particular, we did not detect their accumulation in areas distal to the sheath pocket. Moreover, *vha-5(mc38)* adults rescued by the trafficking mutant transgenes *vha-5(L786S)* or *vha-5(E830Q)* could normally take up DiO (data not shown). Together, these data suggest that the trafficking function of VHA-5 is not essential in amphid sheath cells.

VHA-5 and actin microfilaments are jointly reorganized during molting: The finding that VHA-5 is required for cuticle formation prompted us to examine whether its expression changes during larval molts, as observed for many genes encoding cuticular proteins or proteins involved in their processing (JOHNSTONE 2000; HASHMI *et al.* 2004; FRAND *et al.* 2005; HAO *et al.* 2006). We did not see any major change in VHA-5 abundance during larval stages (not shown); however, we could see that its distribution changed from randomly organized

TABLE 2

Mosaic analysis suggests that *vha-5* is required for viability in the excretory system and, to a lesser extent, in the epidermis

Tissue	Presence of GFP ^a			
	Non-Rdy larvae	Class I Rdy larvae	Class II Rdy larvae	Class III Rdy larvae
Excretory cell	+	–	–	–
Excretory duct cell	+	+	–	–
Epidermis	+	+	+	–
No. of larvae	>600 ^b	5	14	172
Stage 26 hr post-egg laying	Mid-L2	Late L1/young L2	Late L1/young L2	Mid-L1

^a Larvae segregating from *vha-5(mc38); Ex[vha-5::gfp]* transgenic animals were examined for the presence of GFP in the excretory cell, the excretory duct cell, and the epidermis: +, GFP present; –, GFP absent.

^b All larvae expressing the GFP in the excretory system reached adulthood, except two that had very short excretory canals and filled with fluid in late larval development.

spots at intermolts to aligned spots forming parallel circumferential bands at molts (Figure 8 and data not shown). These circumferential bands were strikingly reminiscent of the actin bundles, which disappear after molts and reform prior to molts (COSTA *et al.* 1997). Interestingly, the V1 sector B- and C-subunits of the V-ATPase can bind actin (LEE *et al.* 1999).

To test whether VHA-5 distribution might follow that of actin, we generated a probe to visualize actin *in vivo*. We fused the first 290 residues of the spectraplaklin VAB-10 to YFP (BOSHER *et al.* 2003), since the corresponding domain in human and *Drosophila* VAB-10 homologs is a well-defined actin-binding domain (SUN *et al.* 2001; LEE

and KOŁODZIEJ 2002). This construct, which was driven by the *vha-8* promoter, is described as ABD::YFP in Figure 8 (it was validated as an actin-binding protein using an embryonic epidermal promoter; F. LANDMANN, C. GALLY and M. LABOUESSE, unpublished results). We could thereby correlate changes in actin organization with that of a VHA-5::CFP construct. Consistent with the findings reported by COSTA *et al.* (1997), we observed that actin distribution was disorganized between molts and started to form parallel circumferential filaments slightly before molts (Figure 8). VHA-5 distribution did not correlate with actin between molts, although we assume that the randomly distributed

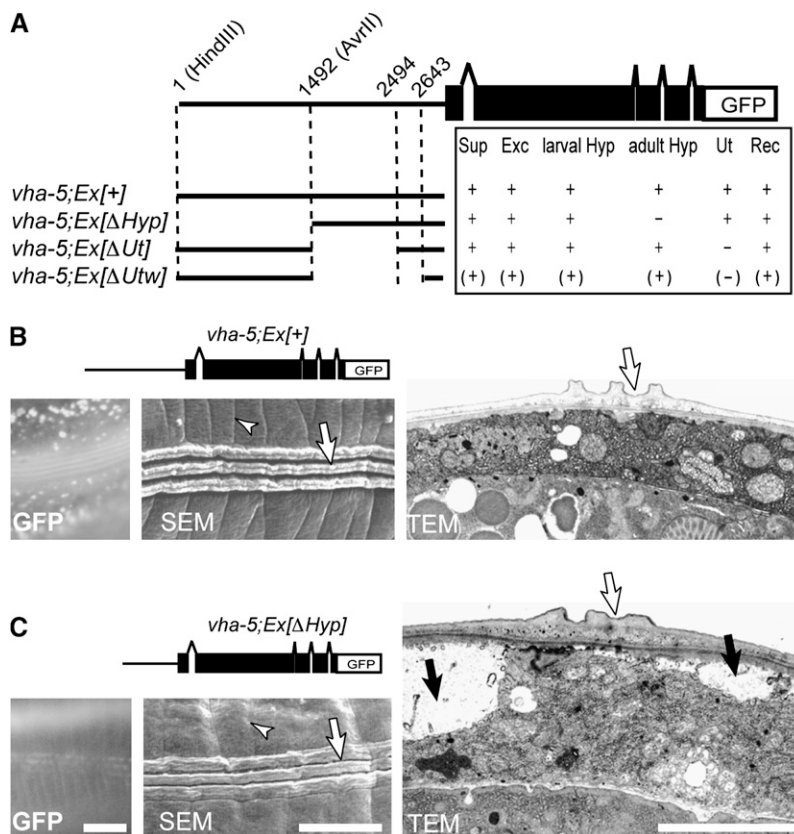


FIGURE 6.—Cell-autonomous activity of *vha-5* in the epidermis. (A) Dissection of the *vha-5* promoter. Each line depicts the promoter sequence (thick line) present upstream from the VHA-5 and GFP coding regions. Expression (+), absence (–), or weak expression (parentheses) of the GFP in tissues where it is normally expressed were assayed: Sup, support cells; Exc, excretory cell; larval Hyp, larval epidermis; adult Hyp, adult epidermis; Ut, uterus; Rec, rectum. (B and C) GFP fluorescence (left), SEM (middle), and TEM (right) micrographs of a *vha-5(mc38)* animal rescued by the control *vha-5::gfp* transgene (pML670, noted *vha-5; Ex[+]*) or by the promoter deletion construct that abrogates GFP expression in the adult epidermis (noted *vha-5; Ex[ΔHyp]*). Note in B the punctate GFP expression in the epidermis (left), the regular annulae (arrowhead in SEM), and the normal alae (arrow in TEM); conversely, note in C the absence of GFP expression in the epidermis (left), the disrupted annulae (arrowhead in SEM), the flat alae (arrow in TEM), and the large vacuoles causing an apparent detachment between the epidermis and the cuticle (solid arrows). Bars, 5 μ m.

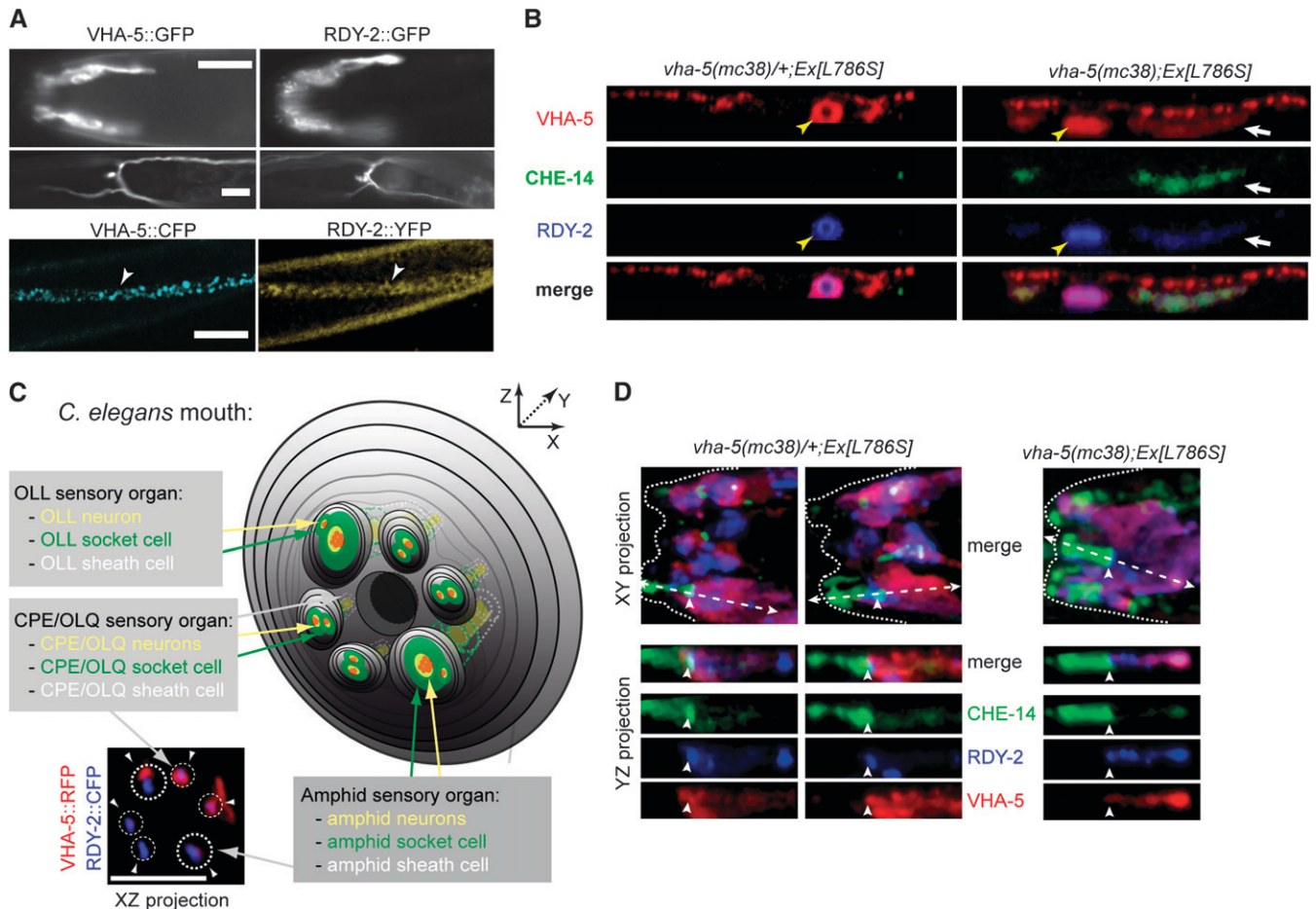


FIGURE 7.—CHE-14, VHA-5, and RDY-2 co-accumulate in the epidermis of *vha-5* mutants affecting secretion but not in their sensory organs. (A) Fluorescence micrographs showing VHA-5::GFP (left) and RDY-2::GFP (right) fusion proteins in different adults (top), or VHA-5::CFP and RDY-2::YFP fusion proteins in the same L2 larva (bottom). Both proteins are expressed in the same tissues, *i.e.*, the amphid sheath cell (top), the excretory cell and canal (middle), the epidermis (bottom, arrowheads). (Top) Lateral view. (Bottom) Ventral views. Bars, 10 μ m. (B) Confocal Z-projections through the epidermis (apical, top of each panel) showing the distributions of CHE-14::YFP and RDY-2::CFP in heterozygous (left) or homozygous (right) *vha-5(mc38)* adults carrying a *vha-5(L786S)::mrfp* mutant transgene (denoted *Ex[L786S]*). All three fluorescent proteins accumulate and colocalize (white arrow) in homozygous *vha-5(mc38)* animals; the *che-14* transgene was generally too weak to be detected in the excretory canal (yellow arrowhead). (C) Scheme of the *C. elegans* mouth (for the sake of simplicity, IL sensory organs are not represented), showing sensory organs where VHA-5 and RDY-2 are expressed. The XZ projection of confocal micrographs (bottom left) shows partial colocalization of VHA-5 and RDY-2 in the apical sheath cells of the amphids (larger dotted circles) and CEP (small dotted circles) and/or in the sheath cells of the OLQ sensory organs (arrowheads); two of the four CEP/OLQ organs seem to have no red signal because it was more difficult to detect them on the other side of the animal. (D) XY projections of confocal micrographs through the head of heterozygous (left) or homozygous (right) *vha-5(mc38)* adults carrying a *vha-5(L786S)::mrfp* mutant transgene, and YZ section through an amphid organ (corresponding to the dotted arrow in the XY projection). CHE-14 was uniquely expressed in the socket cell (to the left of the arrowhead; the sheath cell is to the right of the arrowhead). Five transgenic animals were examined in detail by confocal microscopy. Bars, 5 μ m.

puncta remain linked to the apical plasma membrane (LIÉGEOIS *et al.* 2006). Interestingly, however, at molting VHA-5 puncta became aligned along ABD::YFP-decorated actin bundles and colocalized with them. We conclude that there is a close relationship between secretion of a new cuticle, actin remodeling, and VHA-5-containing V-ATPase distribution.

VHA-5 is required for V-ATPase assembly: The V0 and V1 sectors constantly associate, in which case the V-ATPase proton pump is functional, and dissociate. In yeast, the α -subunit of the V-ATPase is necessary to

assemble the V-ATPase complex (NISHI and FORGAC 2002). To determine whether this might also be the case in *C. elegans*, we visualized the V-ATPase in *rdy* mutants by generating a YFP fusion construct for the V1 sector E-subunit called VHA-8 (CHOI *et al.* 2003). VHA-8::YFP distribution along the excretory canal of *vha-5* null larvae was very diffuse and labeled a much larger area (Figure 9A). Likewise, it was very diffuse in the epidermis of *vha-5* null mutants (Figure 9B) and failed to form the discrete puncta that normally colocalize with VHA-5 in the wild-type epidermis (LIÉGEOIS *et al.* 2006). These

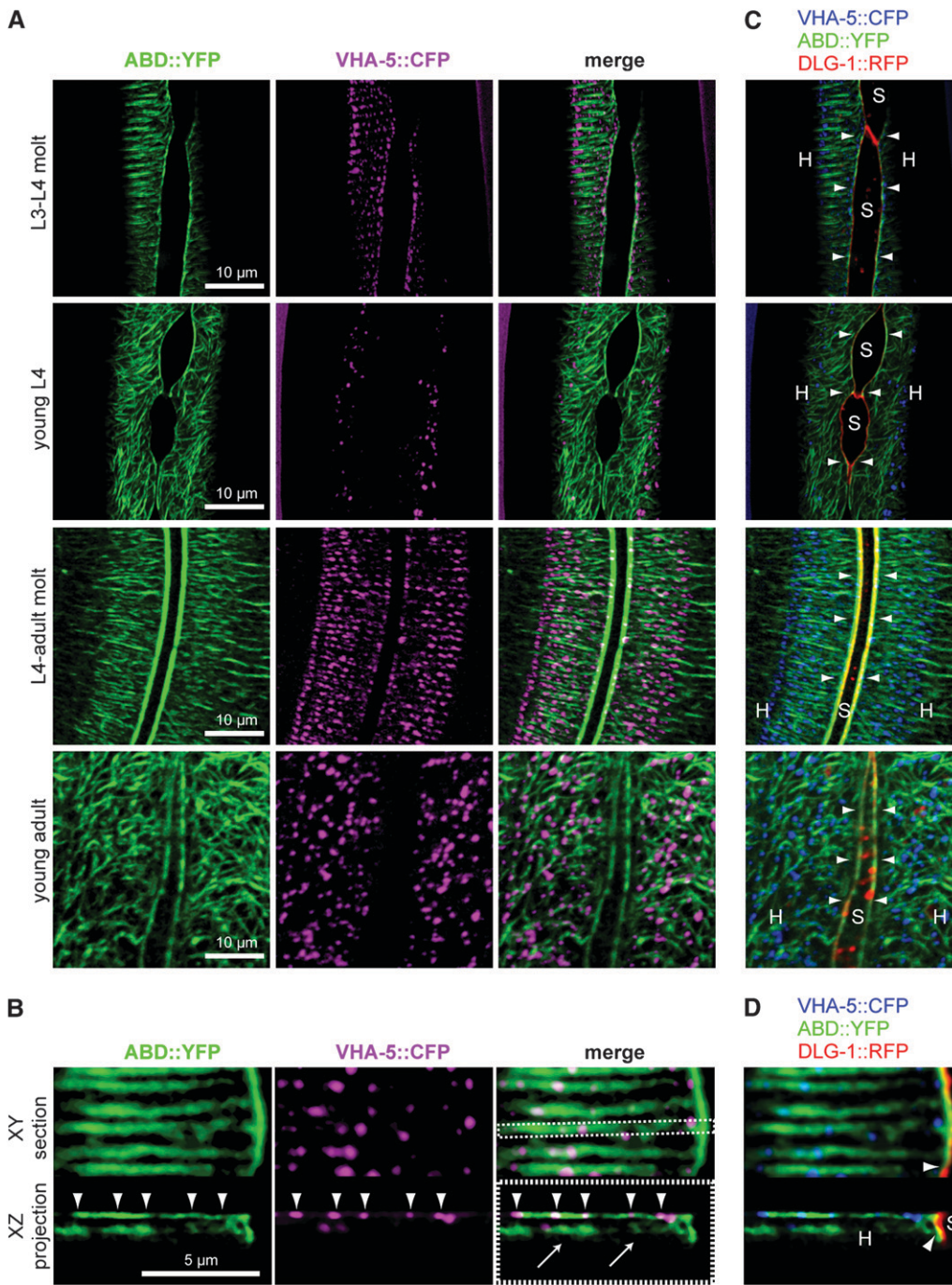


FIGURE 8.—VHA-5 and actin microfilament distributions are jointly reorganized during molting. Confocal micrographs showing the distributions of actin, as revealed by the *vha-8::vab-10_{ABD}::yfp* construct noted ABD::YFP (it corresponds to the actin-binding domain of VAB-10 fused to YFP), VHA-5::CFP, and DLG-1::RFP transgenes at four different time points during larval development. (A) XY projections showing the distributions of actin and VHA-5. Actin microfilaments form parallel bundles during molts (first and third rows), which become disorganized between molts (second and fourth rows). VHA-5 distribution (second column) follows the same pattern, forming aligned dots during molts and dispersed dots in intermolts. Both markers colocalize during molts (merge pictures). (B) Magnification of the apical side of the epidermis during the L4-adult molt when actin bundles are better organized. VHA-5::CFP dots (arrowheads) colocalize with ABD::YFP on the most apical and parallel actin bundles in both XY and XZ projections, rather than on the faint and less organized subapical actin filaments that we reproducibly observed in XZ projections (arrows). (C and D) ABD::YFP bundles surrounding the seam cells (arrowheads) colocalize with DLG-1::RFP at the apical junctions between the hyp7 syncytium (H) and seam cells (S). VHA-5::CFP is shown in violet in A and B (to enhance the contrast) and in blue in C and D.

observations are consistent with our DIC and electron microscopy observations and with results in yeast. In contrast, in *rdy-2* larvae, VHA-8 had a normal distribution along the excretory canal (Figure 9A) and a normal punctate distribution in the epidermis (Figure 9B), suggesting that *rdy-2* is not required for V-ATPase complex formation and/or localization. Using the *vha-8::yfp* reporter, we could also confirm that *rdy-3* mutants had no excretory canal and that the excretory canal of *rdy-4* larvae was not grossly abnormal except for its width (data not shown).

DISCUSSION

Our initial goal was to identify genes acting in the same process as the sterol-sensing domain protein CHE-14 during exocytosis to the apical membrane and/or osmoregulation (MICHAUX *et al.* 2000). The screen identified seven mutations defining four new genes, which share several features with *che-14*, including larval lethality; the failure to absorb lipid dyes such as DiO in chemosensory neurons; and, for six of them, an abnormal cuticle. While mutations displaying one of these

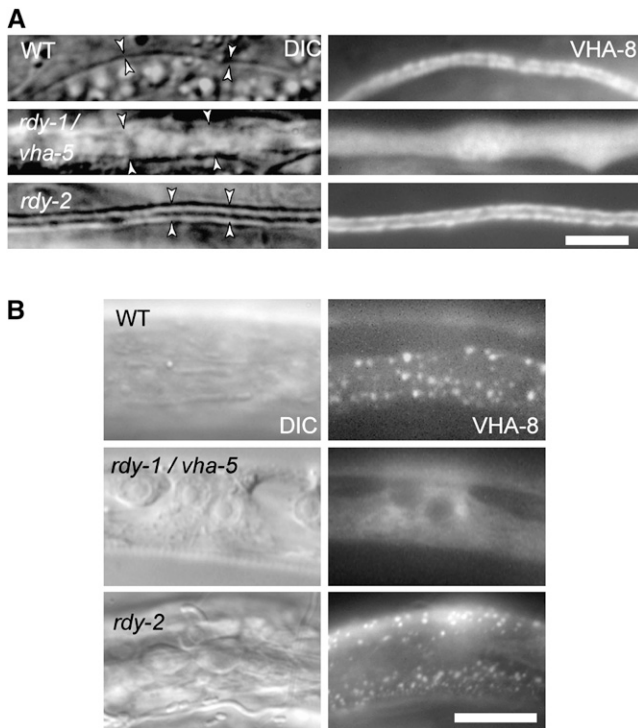


FIGURE 9.—VHA-5 is required for normal assembly of the V-ATPase. DIC and GFP fluorescence views of transgenic larvae expressing a VHA-8::GFP construct; VHA-8 is the VI sector E-subunit. (A) Excretory canal (arrowheads); VHA-8 was very diffuse in *vha-5* larvae. Bar, 2 μm . (B) Epidermis; VHA-8 was also very diffuse in the *vha-5* larva, and the epidermis was vacuolated. Bar, 5 μm .

phenotypes may affect osmoregulation or secretion in a very indirect manner, we reasoned that identifying mutations that combine all three phenotypes should identify genes that play a direct role in osmoregulation and/or secretion. For instance, strong alleles in the Ras pathway lead to rod-like larval lethality because the excretory duct cell adopts another fate (YOCHEM *et al.* 1997), but such dying larvae can still take up DiO (see MATERIALS AND METHODS). Likewise, a search in WormBase (release WS160; <http://www.wormbase.org>) for genes giving dumpy (Dpy), molting (Mlt, indicative of cuticle defects), clear (Clr, indicative of an osmoregulation defect), and larval lethality phenotypes after RNAi identifies only two hits, one of which is *vha-6*. The latter encodes an intestinal V0 α -subunit >65% similar to *vha-5* at the nucleotide level such that short *vha-6* siRNA species might indirectly target *vha-5*. Consistent with the screen being specific, RDY-1/VHA-5 and RDY-2, which we studied further, are like CHE-14 transmembrane proteins found at the apical pole of the three cell types affected in mutants, namely the epidermis, the excretory cell, and support cells.

Despite their phenotypic similarities, there are some notable differences between *che-14* and *vha-5* or *rdy-2*, indicating that they may not act in the same pathway in all cells. First, *che-14* mutations induce a partial lethality

(MICHAX *et al.* 2000), whereas the latter induce complete lethality. Second, large vesicles accumulate in chemosensory sheath cells and amorphous material in the seam cells of *che-14* mutants (PERKINS *et al.* 1986; MICHAX *et al.* 2000), which we did not observe in *vha-5* or *rdy-2* mutants. Finally, CHE-14 is uniquely present in seam cells and socket cells (MICHAX *et al.* 2000). The gene *rdy-3* appears unique in our collection, since it was required for excretory canal formation but not for cuticle assembly. Future work should tell whether *rdy-3* acts primarily to allow excretory lumen extension, as is the case for the chloride channel EXC-4 (BERRY *et al.* 2003), or if it also controls osmoregulation.

VHA-5 exerts different functions in different tissues:

Our molecular identification of *rdy-1* establishes that it corresponds to *vha-5*, which encodes an α -subunit of the V0 sector of the V-ATPase. The V-ATPase has long been known to represent the main enzymatic complex regulating the pH of internal organelles along the endocytic and secretory pathways (NISHI and FORGAC 2002). It is also essential in maintaining osmoregulation in animal excretory systems (SUN-WADA *et al.* 2003), which is entirely consistent with the observation that *vha-5* is expressed in the excretory cell and that its absence leads to dead larvae (see below). Our recent genetic analysis of *vha-5* function in the epidermis (LIÉGEAIS *et al.* 2006) strongly suggests that VHA-5 also has a direct role in secretion. Likewise, biochemical and genetic analyses in yeast and *Drosophila* have suggested that the transmembrane V0 sector of the V-ATPase also has a role in membrane fusion, independently from the cytosolic VI sector and proton pumping (PETERS *et al.* 2001; BAYER *et al.* 2003; HIESINGER *et al.* 2005).

Three observations reported in this work further strengthen the notion that the V0 sector has a direct role in cuticle secretion. First, the null allele *vha-5(mc38)* prevents alae formation, which corroborates previous conclusions based on the analysis of weak alleles (LIÉGEAIS *et al.* 2006). Second, a promoter deletion in a *vha-5* transgene, which rescued larval lethality but prevented expression in the adult epidermis, still induced severe cuticle defects, showing that the absence of alae in *vha-5* null larvae is not an indirect consequence of larval lethality. Third, VHA-5 colocalized with actin microfilaments at the apical surface just prior to molting, suggesting that VHA-5 must form well-organized apical circumferential belts when the bulk of cuticle secretion is at its peak. Actin plays probably multiple, both inhibitory and activating, roles in exocytosis, including a role in positioning exocytotic vesicles (EITZEN 2003). In this framework, we suggest that the V-ATPase subunits B and C, which can bind actin (LEE *et al.* 1999), recruit the V0 sector when actin microfilaments get reorganized ahead of molting to position the V0 sector in circumferential stripes and can subsequently dissociate from the V0 sector, as observed during *Manduca sexta* molting (SUMNER *et al.* 1995). In turn,

we suggest that the V0 sector mediates the secretion of specific cuticle components and thereby contributes to cuticle assembly with its characteristic circumferential annulae. Actin, for instance, might play a role in positioning or allowing the fusion of MVBs, which we showed as playing a key role in cuticle formation (LIÉGEOIS *et al.* 2006). The observation that VHA-5 is necessary for targeting RDY-2 and CHE-14 to the epidermal plasma membrane (Figure 7B) predicts that they should act downstream of VHA-5 in cuticle formation, if they indeed act in the same process. It also suggests that CHE-14 and RDY-2 reach the apical epidermal plasma membrane through MVBs, as previously reported for WRT-2 and WRT-8 (LIÉGEOIS *et al.* 2006).

Two of the phenotypes observed by transmission electron microscopy in neuron-associated sheath cells are similar to those observed in epidermal cells of *vha-5* null larvae. In both cell types, specialized membrane stacks were disorganized and secretion was affected: the granular material surrounding ciliated dendrites was strongly reduced or absent, much like alae were absent and the cuticle abnormal. A key question is whether the secretion defects in sheath cells are due to VHA-5 osmoregulation and pH pumping functions or whether they reflect its direct role in secretion, as in the epidermis. We would argue that it primarily reflects a proton-pumping function, since the *vha-5* point mutation L786S, which affects secretion in the epidermis but not osmoregulation (LIÉGEOIS *et al.* 2006), could normally take up DiO and did not affect RDY-2 or CHE-14 distribution in sheath cells. If this interpretation is correct, it would indicate that the membrane stacks in sheath cells could have a role in osmoregulation rather than in a secretory process as once suspected (PERKINS *et al.* 1986). They could increase the membrane surface for ion exchange as observed in the kidney.

As discussed above, our data thus suggest that VHA-5 trafficking function is central in the epidermis and its osmoregulation function is central in support cells. However, we do not exclude the possibility that VHA-5 also has a minor trafficking role in sheath cells and, conversely, that proton pumping across the epidermal apical membrane by the entire V-ATPase also contributes to epidermal homeostasis. As in support cells, membrane stacks, which are abnormal in *vha-5* mutants (Figure 4B) and where the V-ATPase is present (CHOI *et al.* 2003; LIÉGEOIS *et al.* 2006), could correspond to an osmoregulatory structure. Acidification of the extracellular matrix might facilitate the activity of collagen proconvertases. Interestingly, in many transporting epithelia and in vertebrate osteoclasts, whose main function is to resorb bone collagens, the V-ATPase is enriched at the level of mitochondria-rich membrane invaginations (for review, see BROWN and BRETON 1996; JURDIC *et al.* 2006).

The tetraspan protein RDY-2 has a minor role in secretion: We have shown that RDY-2 is a novel tetraspan

protein with no homology outside of nematodes. The main phenotype of *rdy-2* mutants is an apparent osmoregulation defect, which is similar, albeit slightly less severe, to that of *vha-5* mutants. In addition, we observed that alae were flattened and that the amount of granular material around sensory dendrites was reduced, indicating that its secretory function is also impaired. The RDY-2 protein appeared enriched at the apical membrane, which is compatible with a possible role in apical secretion. However, the absence of clear homology makes it difficult to suggest how it might act molecularly. Other well-characterized tetraspan proteins may provide some clues. Claudins within tight junctions and connexin 32 within gap junctions are involved in cell–cell adhesion, tetraspanins have multiple roles including cell adhesion and membrane integrity, and the small V0 sector ϵ -subunits are proteolipid tetraspan proteins (BRONSTEIN 2000; NISHI and FORGAC 2002). The apical localization of RDY-2 makes it unlikely that it acts in cell adhesion and there was no apparent membrane integrity defect in *rdy-2* mutants. More interestingly, several tetraspan proteins, such as synaptophysin, synaptoporin, synaptogyrin, and MAL/VIP17, have been implicated in vesicle formation or delivery (CHEONG *et al.* 1999; HUBNER *et al.* 2002).

Our preliminary characterization of *rdy-4*, which also has flattened alae, raises the possibility that it might act like *rdy-2*. Further characterization of these two genes should define their precise role in epithelial homeostasis and whether they have, as VHA-5, a direct role in secretion.

Genes involved in osmoregulation and their possible links with trafficking: Our screening procedure identified several genes required for osmoregulation. The finding of a V-ATPase subunit among *rdy*-genes is not surprising, since mutations in the human genes encoding the V1 sector B-subunit and one of the V0 sector α -subunits result in a renal acidification defect, leading to metabolic acidosis (KARET *et al.* 1999; SMITH *et al.* 2000; WAGNER *et al.* 2004), while the excretory cell is considered as the kidney-like organ of the animal (NELSON and RIDDLE 1984). In addition, loss of this B-subunit also leads to sensorineural deafness (KARET *et al.* 1999; SMITH *et al.* 2000), which is presumably linked to a role of the V-ATPase in maintaining the pH of the fluid that surrounds the mechanosensory hair cells (KARET *et al.* 1999). By analogy, it supports our proposal that the enlargement of the sheath pocket surrounding chemosensory neurons observed in *vha-5* null mutants reflects a role of the V-ATPase in maintaining a pH balance in the sheath pocket. Defects in pH maintenance in turn might explain why chemosensory neurons fail to absorb the lipid dye DiO. In organisms that need to rapidly adapt to a changing environment, such as frogs, the V-ATPase plays a key role in maintaining the acid–base balance necessary for Na⁺ uptake in a process that involves hyperpolarization of the external

plasma membrane (EHRENFELD and KLEIN 1997). The free-living nematode *C. elegans* certainly falls in the category of organisms exposed to a rapidly changing environment, which could explain the prominent requirement for the V-ATPase in the excretory cell and epidermis. Our screening strategy and the fact that *vha-5* and *rdy-2* were subsequently found in the excretory system make it quite likely that *rdy-4* also functions in the excretory cell to control osmoregulation.

The V-ATPase is an electrogenic H⁺ pumps that can energize membranes by the voltage component of the proton-motive force rather than by an ionic gradient (WIECZOREK *et al.* 1999). As such, it influences osmoregulation in excretory systems and trafficking pathways, as the pH of both the endocytic and the secretory compartments is tightly controlled (PAROUTIS *et al.* 2004). A few other channels and transporters also contribute to osmoregulation and trafficking, such as chloride channels and sodium/proton antiporters (MARSHANSKY *et al.* 2002). In *C. elegans*, for instance, the epidermal chloride channel gene *clh-1* is required for the formation of alae (PETALCORIN *et al.* 1999), and the intracellular chloride channel EXC-4 is required for extension of the excretory canal lumen by the fusion of smaller vesicles (BERRY *et al.* 2003). The *exc-4* phenotype and the finding that the V0 sector of the V-ATPase promotes membrane fusion in such different systems as yeast vacuoles, *Drosophila* synapses, and the *C. elegans* epidermis, raise the idea that the relationships between ion pump/transporters and membrane fusion are more promiscuous than could have been predicted.

Several rather indirect arguments favor the notion that the apparent link between osmoregulation and trafficking might reflect how the primitive cell acquired membranes and the need to exchange with its environment, rather than the result of evolution being parsimonious and using the same protein for multiple unrelated roles. The potential to secrete ions, waste, and peptides of different sizes might represent a continuum that gradually evolved over time, initially relying on proteins that could create an electrogenic gradient. Regarding the V-ATPase, in some Archaeobacteria, genes encoding subunits of the V0 and V1 sectors are encoded by separate operons (SHIBUI *et al.* 1997), arguing that these two sectors evolved independently before becoming associated within a unique complex and perhaps had different functions in primitive cells. The reversible dissociation of V1 from the V0 sector in modern eukaryotes (NISHI and FORGAC 2002) is consistent with this idea. Furthermore, the genomes of most mycetes have only one V0 α -subunit (CHAVEZ *et al.* 2006), raising the possibility that this subunit originally had the osmoregulation and secretion functions. Hence, the secretion function of the V0 sector might be ancestral among eukaryotes.

We thank Anne Gansmuller [Institut de Génétique et de Biologie Moléculaire et Cellulaire (IGBMC) Imaging Facility] for help with

electron microscopy and Marcel Boeglin and Didier Hentsch (IGBMC Imaging Facility) for help with confocal analysis. We thank Andy Fire, Yuji Kohara, Jeff Hardin, and the Caenorhabditis Genetic Center for reagents. S.L. and A.B. were supported by fellowships from the Ministère de la Recherche and from the Fondation Recherche Médicale. This work was supported by funds from the Centre National de la Recherche Scientifique, Institut National de la Santé et de la Recherche Médicale, and by a grant from the Ministère de la Recherche (programme Action Concertée Incitative).

LITERATURE CITED

- BAYER, M. J., C. REESE, S. BUHLER, C. PETERS and A. MAYER, 2003 Vacuole membrane fusion: V0 functions after trans-SNARE pairing and is coupled to the Ca²⁺-releasing channel. *J. Cell Biol.* **162**: 211–222.
- BERRY, K. L., H. E. BULOW, D. H. HALL and O. HOBERT, 2003 A *C. elegans* CLIC-like protein required for intracellular tube formation and maintenance. *Science* **302**: 2134–2137.
- BOSHER, J. M., B. S. HAHN, R. LEGOUIS, S. SOOKHAREEA, R. M. WEIMER *et al.*, 2003 The Caenorhabditis elegans vab-10 spectraplaklin isoforms protect the epidermis against internal and external forces. *J. Cell Biol.* **161**: 757–768.
- BRENNER, S., 1974 The genetics of *Caenorhabditis elegans*. *Genetics* **77**: 71–94.
- BRETT, C. L., D. N. TUKAYE, S. MUKHERJEE and R. RAO, 2005 The yeast endosomal Na⁺K⁺/H⁺ exchanger Nhx1 regulates cellular pH to control vesicle trafficking. *Mol. Biol. Cell* **16**: 1396–1405.
- BRONSTEIN, J. M., 2000 Function of tetraspan proteins in the myelin sheath. *Curr. Opin. Neurobiol.* **10**: 552–557.
- BROWN, D., and S. BRETON, 1996 Mitochondria-rich, proton-secreting epithelial cells. *J. Exp. Biol.* **199**: 2345–2358.
- BURKE, R., D. NELLEN, M. BELLOTTO, E. HAFEN, K. A. SENTI *et al.*, 1999 Dispatched, a novel sterol-sensing domain protein dedicated to the release of cholesterol-modified hedgehog from signaling cells. *Cell* **99**: 803–815.
- CHAVEZ, C., E. J. BOWMAN, J. C. REIDLING, K. H. HAW and B. J. BOWMAN, 2006 Analysis of strains with mutations in six genes encoding subunits of the V-ATPase: eukaryotes differ in the composition of the V0 sector of the enzyme. *J. Biol. Chem.* **281**: 27052–27062.
- CHEONG, K. H., D. ZACCHETTI, E. E. SCHNEEBERGER and K. SIMONS, 1999 VIP17/MAL, a lipid raft-associated protein, is involved in apical transport in MDCK cells. *Proc. Natl. Acad. Sci. USA* **96**: 6241–6248.
- CHOI, K. Y., Y. J. JI, B. K. DHAKAL, J. R. YU, C. CHO *et al.*, 2003 Vacuolar-type H⁺-ATPase E subunit is required for embryogenesis and yolk transfer in *Caenorhabditis elegans*. *Gene* **311**: 13–23.
- COSTA, M., B. W. DRAPER and J. R. PRIESS, 1997 The role of actin filaments in patterning the *Caenorhabditis elegans* cuticle. *Dev. Biol.* **184**: 373–384.
- EHRENFELD, J., and U. KLEIN, 1997 The key role of the H⁺ V-ATPase in acid-base balance and Na⁺ transport processes in frog skin. *J. Exp. Biol.* **200**: 247–256.
- EITZEN, G., 2003 Actin remodeling to facilitate membrane fusion. *Biochim. Biophys. Acta* **1641**: 175–181.
- FIRE, A., S. XU, M. K. MONTGOMERY, S. A. KOSTAS, S. E. DRIVER *et al.*, 1998 Potent and specific genetic interference by double-stranded RNA in *Caenorhabditis elegans*. *Nature* **391**: 806–811.
- FRAND, A. R., S. RUSSEL and G. RUVKUN, 2005 Functional genomic analysis of *C. elegans* molting. *PLoS Biol.* **3**: e312.
- HAO, L., K. MUKHERJEE, S. LIEGEOS, D. BAILLIE, M. LABOUESSE *et al.*, 2006 The hedgehog-related gene *qua-1* is required for molting in *Caenorhabditis elegans*. *Dev. Dyn.* **235**: 1469–1481.
- HASHMI, S., J. ZHANG, Y. ORSOV and S. LUSTIGMAN, 2004 The *Caenorhabditis elegans* cathepsin Z-like cysteine protease, Ce-CPZ-1, has a multifunctional role during the worms' development. *J. Biol. Chem.* **279**: 6035–6045.
- HIESINGER, P. R., A. FAYYAZUDDIN, S. Q. MEHTA, T. ROSENMUND, K. L. SCHULZE *et al.*, 2005 The v-ATPase V0 subunit $\alpha 1$ is required

- for a late step in synaptic vesicle exocytosis in *Drosophila*. *Cell* **121**: 607–620.
- HOHMANN, S., 2002 Osmotic stress signaling and osmoadaptation in yeasts. *Microbiol. Mol. Biol. Rev.* **66**: 300–372.
- HUBNER, K., R. WINDOFFER, H. HUTTER and R. E. LEUBE, 2002 Tetraspan vesicle membrane proteins: synthesis, subcellular localization, and functional properties. *Int. Rev. Cytol.* **214**: 103–159.
- JOHNSTONE, I. L., 2000 Cuticle collagen genes: expression in *Caenorhabditis elegans*. *Trends Genet.* **16**: 21–27.
- JORGENSEN, E. M., and S. E. MANGO, 2002 The art and design of genetic screens: *Caenorhabditis elegans*. *Nat. Rev. Genet.* **3**: 356–369.
- JURDIC, P., F. SALTTEL, A. CHABADEL and O. DESTAING, 2006 Podosome and sealing zone: specificity of the osteoclast model. *Eur. J. Cell Biol.* **85**: 195–202.
- KAITNA, S., H. SCHNABEL, R. SCHNABEL, A. A. HYMAN and M. GLOTZER, 2002 A ubiquitin C-terminal hydrolase is required to maintain osmotic balance and execute actin-dependent processes in the early *C. elegans* embryo. *J. Cell Sci.* **115**: 2293–2302.
- KARET, F. E., K. E. FINBERG, R. D. NELSON, A. NAYIR, H. MOCAN *et al.*, 1999 Mutations in the gene encoding B1 subunit of H⁺-ATPase cause renal tubular acidosis with sensorineural deafness. *Nat. Genet.* **21**: 84–90.
- LAMITINA, S. T., and K. STRANGE, 2005 Transcriptional targets of DAF-16 insulin signaling pathway protect *C. elegans* from extreme hypertonic stress. *Am. J. Physiol. Cell Physiol.* **288**: C467–C474.
- LEE, B. S., S. L. GLUCK and L. S. HOLLIDAY, 1999 Interaction between vacuolar H⁽⁺⁾-ATPase and microfilaments during osteoclast activation. *J. Biol. Chem.* **274**: 29164–29171.
- LEE, S., and P. A. KOLODZIEJ, 2002 The plakin Short Stop and the RhoA GTPase are required for E-cadherin-dependent apical surface remodeling during tracheal tube fusion. *Development* **129**: 1509–1520.
- LIÉGEOIS, S., A. BENEDETTO, J. M. GARNIER, Y. SCHWAB and M. LABOUESSE, 2006 The V0-ATPase mediates apical secretion of exosomes containing Hedgehog-related proteins in *Caenorhabditis elegans*. *J. Cell Biol.* **173**: 949–961.
- MARSHANSKY, V., D. A. AUSIELLO and D. BROWN, 2002 Physiological importance of endosomal acidification: potential role in proximal tubulopathies. *Curr. Opin. Nephrol. Hypertens.* **11**: 527–537.
- MELLO, C. C., J. M. KRAMER, D. STINCHCOMB and V. AMBROS, 1991 Efficient gene transfer in *C. elegans*: extrachromosomal maintenance and integration of transforming sequences. *EMBO J.* **10**: 3959–3970.
- MICHAUX, G., A. GANSMULLER, C. HINDELANG and M. LABOUESSE, 2000 CHE-14, a protein with a sterol-sensing domain, is required for apical sorting in *C. elegans* ectodermal epithelial cells. *Curr. Biol.* **10**: 1098–1107.
- NELSON, F. K., and D. L. RIDDLE, 1984 Functional study of the *Caenorhabditis elegans* secretory-excretory system using laser microsurgery. *J. Exp. Zool.* **231**: 45–56.
- NIELSEN, S., S. R. DIGIOVANNI, E. I. CHRISTENSEN, M. A. KNEPPER and H. W. HARRIS, 1993 Cellular and subcellular immunolocalization of vasopressin-regulated water channel in rat kidney. *Proc. Natl. Acad. Sci. USA* **90**: 11663–11667.
- NIELSEN, S., C. L. CHOU, D. MARPLES, E. I. CHRISTENSEN, B. K. KISHORE *et al.*, 1995 Vasopressin increases water permeability of kidney collecting duct by inducing translocation of aquaporin-CD water channels to plasma membrane. *Proc. Natl. Acad. Sci. USA* **92**: 1013–1017.
- NISHI, T., and M. FORGAC, 2002 The vacuolar (H⁺)-ATPases: nature's most versatile proton pumps. *Nat. Rev. Mol. Cell Biol.* **3**: 94–103.
- NURRISH, S. J., 2002 An overview of *C. elegans* trafficking mutants. *Traffic* **3**: 2–10.
- OKA, T., T. TOYOMURA, K. HONJO, Y. WADA and M. FUTAI, 2001 Four subunit isoforms of *Caenorhabditis elegans* vacuolar H⁺-ATPase. Cell-specific expression during development. *J. Biol. Chem.* **276**: 33079–33085.
- PAROUTIS, P., N. TOURET and S. GRINSTEIN, 2004 The pH of the secretory pathway: measurement, determinants, and regulation. *Physiology (Bethesda)* **19**: 207–215.
- PERKINS, L. A., E. M. HEDGECOCK, J. N. THOMSON and J. G. CULOTTI, 1986 Mutant sensory cilia in the nematode *Caenorhabditis elegans*. *Dev. Biol.* **117**: 456–487.
- PETALCORIN, M. I., T. OKA, M. KOGA, K. OGURA, Y. WADA *et al.*, 1999 Disruption of *clh-1*, a chloride channel gene, results in a wider body of *Caenorhabditis elegans*. *J. Mol. Biol.* **294**: 347–355.
- PETERS, C., M. J. BAYER, S. BUHLER, J. S. ANDERSEN, M. MANN *et al.*, 2001 Trans-complex formation by proteolipid channels in the terminal phase of membrane fusion. *Nature* **409**: 581–588.
- PUJOL, N., C. BONNEROT, J. J. EWBANK, Y. KOHARA and D. THIERRY-MIEG, 2001 The *Caenorhabditis elegans unc-32* gene encodes alternative forms of a vacuolar ATPase a subunit. *J. Biol. Chem.* **276**: 11913–11921.
- SAPIO, M. R., M. A. HILLIARD, M. CERMOLA, R. FAVRE and P. BAZZICALUPO, 2005 The zona pellucida domain containing proteins, CUT-1, CUT-3 and CUT-5, play essential roles in the development of the larval alae in *Caenorhabditis elegans*. *Dev. Biol.* **282**: 231–245.
- SHEKMAN, R., and P. NOVICK, 2004 23 genes, 23 years later. *Cell* **116**: S13–S15.
- SHIBUI, H., T. HAMAMOTO, M. YOHDA and Y. KAGAWA, 1997 The stabilizing residues and the functional domains in the hyperthermophilic V-ATPase of *Desulfurococcus*. *Biochem. Biophys. Res. Commun.* **234**: 341–345.
- SMITH, A. N., J. SKAUG, K. A. CHOATE, A. NAYIR, A. BAKKALOGLU *et al.*, 2000 Mutations in ATP6N1B, encoding a new kidney vacuolar proton pump 116-kD subunit, cause recessive distal renal tubular acidosis with preserved hearing. *Nat. Genet.* **26**: 71–75.
- SOLOMON, A., S. BANDHAKAVI, S. JABBAR, R. SHAH, G. J. BEITEL *et al.*, 2004 *Caenorhabditis elegans* OSR-1 regulates behavioral and physiological responses to hyperosmotic environments. *Genetics* **167**: 161–170.
- SUMNER, J. P., J. A. DOW, F. G. EARLEY, U. KLEIN, D. JAGER *et al.*, 1995 Regulation of plasma membrane V-ATPase activity by dissociation of peripheral subunits. *J. Biol. Chem.* **270**: 5649–5653.
- SUN, D., C. L. LEUNG and R. K. LIEM, 2001 Characterization of the microtubule binding domain of microtubule actin crosslinking factor (MACF): identification of a novel group of microtubule associated proteins. *J. Cell Sci.* **114**: 161–172.
- SUN-WADA, G. H., Y. WADA and M. FUTAI, 2003 Lysosome and lysosome-related organelles responsible for specialized functions in higher organisms, with special emphasis on vacuolar-type proton ATPase. *Cell Struct. Funct.* **28**: 455–463.
- WAGNER, C. A., K. E. FINBERG, S. BRETON, V. MARSHANSKY, D. BROWN *et al.*, 2004 Renal vacuolar H⁺-ATPase. *Physiol. Rev.* **84**: 1263–1314.
- WICKS, S. R., R. T. YEH, W. R. GISH, R. H. WATERSTON and R. H. PLASTERK, 2001 Rapid gene mapping in *Caenorhabditis elegans* using a high density polymorphism map. *Nat. Genet.* **28**: 160–164.
- WIECZOREK, H., D. BROWN, S. GRINSTEIN, J. EHRENFELD and W. R. HARVEY, 1999 Animal plasma membrane energization by proton-motive V-ATPases. *BioEssays* **21**: 637–648.
- WILLIAMS, B. D., B. SCHRANK, C. HUYNH, R. SHOWNKEEN and R. H. WATERSTON, 1992 A genetic mapping system in *Caenorhabditis elegans* based on polymorphic sequence-tagged sites. *Genetics* **131**: 609–624.
- YANCEY, P. H., M. E. CLARK, S. C. HAND, R. D. BOWLUS and G. N. SOMERO, 1982 Living with water stress: evolution of osmolyte systems. *Science* **217**: 1214–1222.
- YOCHEM, J., M. SUNDARAM and M. HAN, 1997 Ras is required for a limited number of cell fates and not for general proliferation in *Caenorhabditis elegans*. *Mol. Cell. Biol.* **17**: 2716–2722.
- ZHU, J., R. J. HILL, P. J. HEID, M. FUKUYAMA, A. SUGIMOTO *et al.*, 1997 *end-1* encodes an apparent GATA factor that specifies the endoderm precursor in *Caenorhabditis elegans* embryos. *Genes Dev.* **11**: 2883–2896.